PALEOCEANOGRAPHY, VOL. 5, NO. 4, PAGES 557-580, AUGUST 1990

SURFACE SEDIMENT DIATOM DISTRIBUTION AND HOLOCENE PALEOTEMPERATURE VARIATIONS IN THE GREENLAND, ICELAND AND NORWEGIAN SEA

Nalân Koc Karpuz and Hans Schrader

Geological Institute, University of Bergen,
Bergen, Norway

Abstract. One hundred and four surface sediment samples and two piston cores from the Greenland, Iceland and the Norwegian (GIN) Sea (Hopkins, 1988) were analyzed. Diatoms were common to abundant in most surface sediment samples and throughout the Holocene. Q mode factor analysis allowed the definition of six significantly different floral assemblages which explained 91.7% of the total variance. Mapping of the six factors showed their close affinity to hydrographic regimes. These are the Norwegian-Atlantic Current assemblage (*Thalassionema nitzschioides, Paralia sulcata, Proboscia alata*), Arctic Water assemblage (*Thalassiosira gravida* spores), Sea Ice assemblage (*Nitzschia grunowii, Nitzschia cylindra, Thalassiosira hyalina*), Arctic-Norwegian Waters Mixing assemblage (*Rhizosolenia hebetata f. semispina, Rhizosolenia borealis*), Atlantic assemblage (*Thalassiosira oestrupii*), and Norwegian-Arctic Waters Mixing assemblage (*Thalassiosira gravida* vegetative cells). Transfer functions (GINT2) relating factor distributions to winter (February) and summer (August) surface water temperatures were generated. The transfer functions have a standard error of estimate of $\pm 1.5^{\circ}$C (August) and $\pm 1.0^{\circ}$C (February). Downcore studies of core 52-43 from the Norwegian Basin and core 57-5 from the Iceland Plateau revealed diatom abundance and sea surface paleotemperature trends in the area during the Holocene. The first appearance of diatoms in cores 52-43 and 57-5 occurs within the Vedde ash layer (10,600 years B.P.) and the Saksunarvatn ash layer (9100 years B.P.), respectively. Diatom abundances increase steadily throughout the Pre-Boreal-Atlantic time to 25 and 35 million valves per gram dry sediment in the Norwegian Basin and Iceland Plateau cores, respectively. Application of the temperature transfer functions (GINT2) to the two Holocene records revealed higher than present sea surface temperatures during the Boreal-Atlantic chronozones for the Iceland Plateau and during the middle Younger Dryas-Sub Boreal chronozones for the Norwegian Basin core. Temperatures decreased steadily since then with a slight increase to the present values. Both the Iceland and the Norwegian seas experienced a strong influx of temperate Atlantic surface waters in the beginning of the Holocene. Sea surface temperatures dropped steadily in the latter part of the Holocene as the influx of the Atlantic surface waters diminished.

Paper number 90PA01227.
0883-8305/90/90PA-01227$10.00

INTRODUCTION

The influence of warm North Atlantic surface waters (Figure 1) on the continental and oceanic climate of NW Europe and the northern high-latitude ocean is undeniable. North Atlantic surface waters have been present only twice in the Norwegian Sea during the last 220,000 years, namely, during oxygen isotope stages 5e and 1 [Kellogg, 1975; Ruddiman and McIntyre, 1976]. Both the continental and the oceanic climate changed drastically each time warm North Atlantic waters intruded into the cold and ice-laden waters of the north. Increased temperatures and high salinities caused total paleobiotic change from a predominantly Arctic to a Boreal assemblage [Thomsen and Vorren, 1986; Jansen and Bjørklund, 1985].

Late Quaternary intrusion of North Atlantic surface waters into the eastern Norwegian Sea took place about 13,000 years B.P. [Jansen et al., 1983]. A temporary retreat of the North Atlantic waters during the Younger Dryas

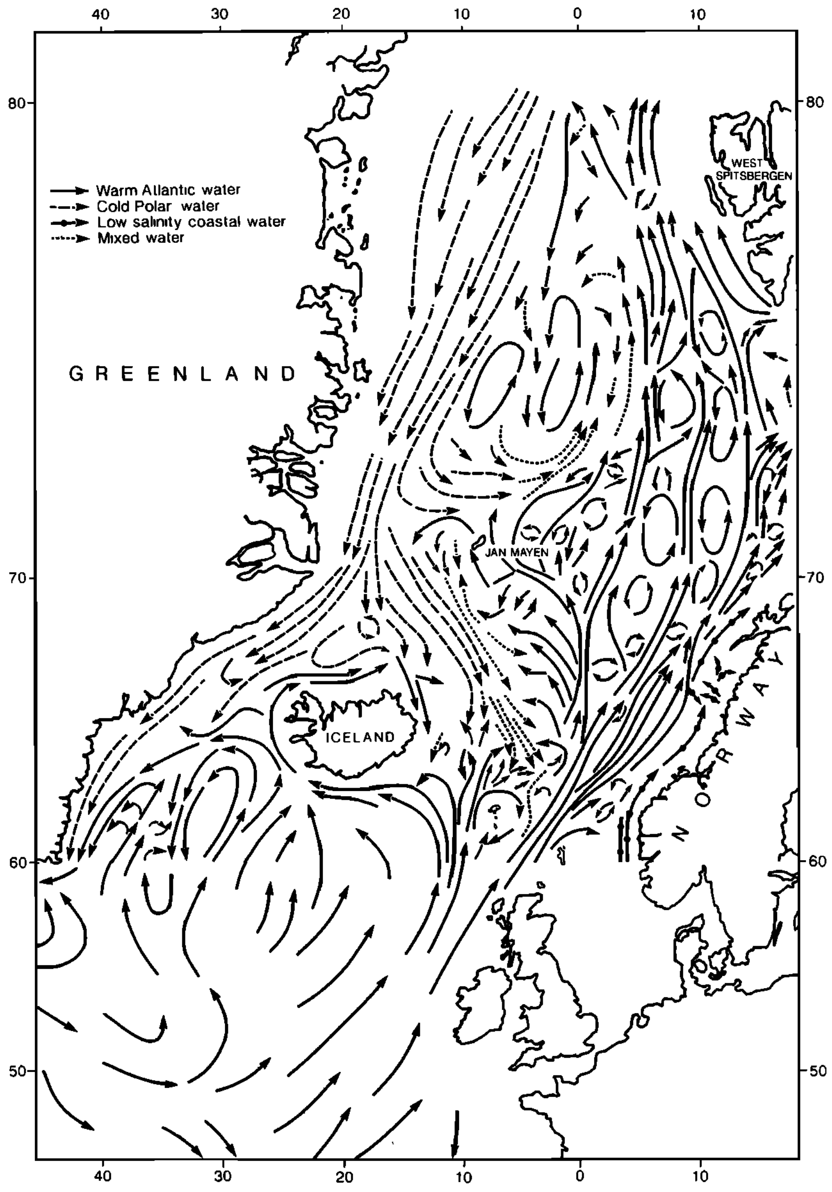

Fig. 1. Surface currents in the GIN Sea and the North Atlantic from Alekseev and Istochin [1956].

(11,000-10,000 years B.P. [Ruddiman and McIntyre, 1981; Jansen and Bjørklund; 1985; Mangerud, 1987; Fairbanks, 1989]) produced a short episode of cold climate in the northern high latitudes. The Younger Dryas/Holocene transition in marine sediments is marked by a rise in the carbonate percentages and an increase in abundance of the subpolar planktonic foraminifer *Neogloboquadrina pachyderma* (right coiling). This event is centered on or just above the youngest ash zone in the North Atlantic deep-sea cores [Ruddiman and McIntyre, 1981]. This North Atlantic ash zone together with the Greenland, Iceland and Norwegian (GIN) Sea ash zone is correlated [Sjøholm, 1988; Kvamme et al., 1989] to the Vedde ash zone (10,600 years B.P.) of western Norway [Mangerud et al., 1984]. Assuming a synchronous deposition of the ash, warming of the Atlantic waters started around 10,600 years B.P. in the North Atlantic and the Norwegian Sea.

The purpose of this study is to analyze the Holocene sea surface temperature (SST) variations in two cores from the Norwegian and Iceland seas using marine diatom sediment assemblages. Marine planktonic diatoms are photosynthetic and single-celled siliceous algae. They constitute the major part of the phytoplankton, together with coccolithophorids and flagellates, of the world ocean and are primary producers. Diatoms, being phytoplankton are dependent on light, and thus they inhibit the upper 100 m of the water column. Salinity and temperature variations of the surface waters present barriers to the biogeographical distribution of some species. Otherwise, as a group they have very large salinity and temperature tolerances. The high-latitude species diversity is also high (43 major species in this study) [Sancetta, 1982; Schrader and Koc Karpuz, 1990].

Sea ice has been an important component of the physical environment in high latitudes. A special ice algal community dominated by diatoms thrives in the ice and in the waters of the marginal ice zone [Horner, 1985]. Therefore, this group of microfossils can give detailed information on paleo-sea surface temperature, sea surface salinity, sea ice cover, and productivity.

This paper builds on results presented by Schrader and Koc Karpuz [1990] by expanding the distribution of surface samples to cover larger biogeographic areas and resolving possible sea ice relationships in the northern and western parts of the GIN Sea and the North Atlantic. The resulting transfer functions thus differs from that of Schrader and Koc Karpuz [1990] by including larger temperature ranges. Additionally, two Holocene records, one from the Iceland Plateau and one from the eastern Norwegian Basin, are analyzed in this paper.

MATERIAL

One hundred and four surface sediment samples and two piston cores from the GIN Sea were analyzed in this study. The location, depth, average winter and summer temperatures, diatom abundances, and repositories of the surface sediment samples are listed in Table 1, and their position is drafted in Figure 2. The areal coverage of surface sediment samples is good over the Iceland Plateau and the Norwegian Basin and poor over the Lofoten and Greenland basins and the North Atlantic; therefore more interpolation between sparse sample coverage was done.

Two piston cores were selected for the Holocene downcore diatom study; one from the Iceland Plateau (57-5) and the other from the Norwegian Basin (52-43) (Figure 8 and Table 2). The location of these two cores permits an east to west paleoclimatic variation comparison in the GIN Sea. Core 57-5 was selected because of its central position on the Iceland Plateau. The sedimentological and the oxygen isotope analyses of the planktonic foraminifera had been previously done [Beyer, 1988]. Quaternary tephrachronology and geochemistry of the ash layers were investigated by Sjøholm [1987]. On the basis of geochemical analysis she concluded that the upper ash zone contains one rhyolitic and one transitional alkalic basaltic ash population which can be correlated with the Vedde ash (10,600 years B.P.) and a second tholeiitic basaltic population which she correlated with the Saksunarvatn ash (9100 years B.P.). On the basis of the Saksunarvatn ash layer a sedimentation rate of 2.1 cm/1000 years was calculated for the Holocene. This sedimentation rate is characteristic for the Holocene period of the Iceland Plateau. Today, core 57-5 is located under the seasonally sea ice covered Arctic waters.

Core 52-43 was collected from the Norwegian Basin (Figure 8). Sedimentological analyses were done by Befring [1984]. Oxygen isotope and faunal studies of planktonic and benthic foraminifera analyses were carried out by T. Veum (unpublished data, 1989). The ash zone situated at a 47.5-50 cm depth interval and dominated by thin, platy, colorless, rhyolitic grains was correlated to the Vedde ash (10,600 years B.P.). Interpolation of the age between the Vedde ash layer and the present resulted in a sedimentation rate of 4.5 cm/1000 years (Table 2), assuming a constant sedimentation rate during the time interval in question. Results of the radiocarbon dated *Neogloboquadrina pachyderma* (right coiling) (E. Jansen, personal communication, 1990) by accelerator mass spectrometry (AMS) from the core support the correlation to the Vedde ash layer and the proposed time scale. Today, the core lies under the path of the northward flowing warm and saline North Atlantic waters. Therefore, this core is in a position to record changes taking place in the influx of the North Atlantic waters to the GIN Sea.

METHODS

The cores were continuously channel sampled in adjacent 2.5-cm sections to provide a complete record over the time interval studied. Midpoints of these channel samples are used in the figures. Both the surface and the downcore initial samples of 0.5 g were cleaned according to the method of Abelmann [1988]. A fractionated settling technique was applied to the samples to eliminate the clay fraction and to concentrate the diatom frustules. Quantitative diatom slides from aliquots of cleaned samples were prepared by homogenizing an aliquot in 25 mL distilled water and pouring it into a petri dish which contained three cover slips covered with photo flow and gelatine solution (R. Gersonde, personal communication, 1988). A settling time of 2 hours was allowed before placing a paper towel into the side of the dish for sucking out the overstanding water. After the material had completely dried, cover slips were then transfered onto a hot plate under the hood and mounted with a high refractive index medium onto permanently labeled slides. At least 400 diatom frustules (on a *Chaetoceros* free basis) from each sample were counted on random traverses at 1320x magnification using the counting procedures of Schrader and Gersonde [1978]. Diatom abundances (number of valves per gram dry sediment) were calculated for both the surface sediment samples (Table 1) and the two Holocene records (Tables 3 and 4).

A total of 43 taxonomic entities were distinguished; the taxonomic interpretations followed those of Fryxell and Hasle [1972, 1980], Hustedt [1930, 1959], Hasle [1978], Hasle and Fryxell [1977], Sancetta [1982], Simonsen [1974], Sundström [1986], and Syvertsen [1979].

The statistical methods of Imbrie and Kipp [1971] were applied to the raw data set. CABFAC Q mode factor analysis, THREAD pseudofactor analysis, and REGRESS stepwise multiple regression programs were used.

RESULTS

The Present

Out of the total 104 surface samples, 87 were used in the Q mode factor analysis (see Table 1); 17 surface samples

TABLE 1. Location, Source, Temperature, and Diatom Valve Abundance of 104 Surface Sediment Samples

Sample[a]	Station[b]	Position		Water Depth	Surface Water Temperatures,[c] °C		Diatom Abundance[d]
		Latitude	Longitude	m	August	February	
1	21302 K	78° 37.0′ N	11° 02.1′ W	175	-1.7	-1.7	1.8
2	21300 K	77° 59.9′ N	04° 44.1′ W	1778	-1.1	-1.7	barren
3	21299 K	77° 59.2′ N	04° 16.7′ W	2404	0.3	-1.7	barren
4	21298 K	78° 00.0′ N	03° 01.0′ W	2745	3.1	-1.7	9.0
5	21297 K	77° 59.8′ N	01° 02.8′ W	3051	3.3	-1.7	2.6
6	21296 K	78° 00.1′ N	00° 37.5′ E	3101	3.8	-1.7	4.0
7	21295 K	77° 59.8′ N	02° 27.8′ E	3112	4.2	-1.7	10.1
8	21294 K	78° 00.2′ N	05° 21.9′ E	2677	5.1	-1.1	3.4
9	21293 K	77° 59.8′ N	06° 40.5′ E	2462	5.5	0.4	30.4
10	21292 K	77° 59.8′ N	07° 25.0′ E	3536	5.8	1.1	44.0
11	21291 K	78° 00.4′ N	08° 04.0′ E	2400	5.9	1.7	35.2
12	ArkV-131K	74° 24.4′ N	17° 32.3′ W	236	-1.7	-1.7	barren
13	ArkV-125K	74° 10.6′ N	14° 34.1′ W	877	-1.7	-1.7	barren
14	ArkV-147K	74° 13.8′ N	10° 02.3′ W	3150	1.3	-1.7	6.5
15	ArkV-129K	72° 39.9′ N	17° 50.4′ W	279	-1.7	-1.7	barren
16	ArkV-149K	72° 37.0′ N	13° 50.4′ W	2118	-1.1	-1.7	4.3
17	23338 K	72° 35.7′ N	10° 29.5′ W	2240	2.4	-1.7	3.8
18	23294 K	72° 22.8′ N	01° 35.5′ W	2224	5.8	0.3	barren
19	23343 K	72° 12.8′ N	12° 59.7′ W	2400	1.0	-1.7	3.7
20	23344 K	71° 44.1′ N	15° 34.8′ W	1093	-1.1	-1.7	3.6
21	23345 K	71° 40.1′ N	14° 19.0′ W	1385	0.3	-1.7	2.9
22	ArkV-150K	71° 48.7′ N	12° 34.2′ W	1298	1.9	-1.7	barren
23	23342 K	71° 37.8′ N	08° 24.8′ W	1958	4.4	-1.7	3.1
24	23346 K	71° 17.5′ N	14° 03.9′ W	1213	1.7	-1.7	7.1
25	23349 K	70° 23.3′ N	20° 11.4′ W	308	-1.1	-1.7	5.1
26	23350 K	70° 23.8′ N	19° 20.8′ W	400	0.3	-1.7	3.8
27	23348 K	70° 25.1′ N	18° 56.9′ W	729	0.3	-1.7	3.4
28	23351 K	70° 21.7′ N	18° 12.3′ W	1673	1.0	-1.7	1.0
29	71-14 B	69° 58.6′ N	18° 05.4′ W	1624	0.1	-1.7	1.0
30	23347 K	70° 26.2′ N	16° 04.8′ W	1229	2.8	-1.7	3.1
31	23353 K	70° 34.2′ N	12° 43.4′ W	1404	3.8	-1.7	7.5
32	23354 K	70° 19.8′ N	10° 37.7′ W	1747	5.0	-1.1	15.1
33	23295 K	71° 08.1′ N	05° 59.2′ W	1553	5.5	0.3	20.6
34	23341 K	70° 57.0′ N	05° 32.6′ W	1734	5.9	1.1	5.8
35	71-17 B	70° 00.4′ N	13° 01.1′ W	1460	4.4	-1.1	27.3
36	23352 K	70° 00.4′ N	12° 25.4′ W	1823	5.0	-1.1	11.4
37	71-20 B	70° 04.2′ N	06° 52.7′ W	2005	6.2	1.7	2.7
38	23059 K	70° 18.4′ N	03° 06.4′ W	2285	7.2	2.5	6.7
39	23337 K	70° 03.2′ N	00° 03.5′ E	3296	9.3	4.4	5.4
40	57-06 B	69° 27.2′ N	14° 32.3′ W	1458	5.4	-0.6	16.0
41	57-05 B	69° 08.3′ N	13° 07.2′ W	1892	5.6	0.7	24.6
42	71-19 B	69° 29.0′ N	09° 30.6′ W	2210	6.0	0.7	9.1
43	71-21 B	69° 57.3′ N	06° 09.7′ W	2612	6.8	1.9	6.9
44	71-22 B	69° 20.1′ N	03° 37.1′ W	1833	8.6	3.1	2.8
45	71-12 B	68° 25.7′ N	13° 52.2′ W	1633	6.7	-0.6	23.1
46	V30-130 L	67° 30.0′ N	15° 04.0′ W	858	6.7	2.0	65.0
47	57-08 B	68° 10.3′ N	11° 32.4′ W	1953	6.6	1.6	23.1
48	57-04 B	68° 31.9′ N	10° 39.9′ W	2122	7.0	1.6	20.4
49	57-09 B	67° 29.9′ N	11° 39.6′ W	1662	6.6	-0.9	18.0
50	57-10 B	67° 00.3′ N	09° 18.5′ W	1485	6.6	2.1	15.8
51	57-12 B	67° 04.8′ N	07° 18.8′ W	2093	8.6	1.6	14.0
52	57-14 B	66° 59.8′ N	06° 12.3′ W	3005	8.8	2.7	8.8
53	71-25 B	67° 59.8′ N	00° 14.0′ E	2850	11.3	5.8	12.3
54	23065 K	68° 30.0′ N	00° 49.9′ E	2796	10.8	5.1	6.2
55	23056 K	68° 30.1′ N	03° 30.3′ E	2665	11.4	5.8	12.7

TABLE 1. (continued)

Sample[a]	Station[b]	Position		Water Depth	Surface Water Temperatures,[c] °C		Diatom Abundance[d]
		Latitude	Longitude	m	August	February	
56	23334 K	68° 40.4′ N	05° 56.1′ E	3003	11.1	6.1	3.4
57	23055 K	68° 25.2′ N	04° 00.3′ E	2298	11.4	6.1	12.8
58	23335 K	67° 40.4′ N	05° 49.9′ E	1395	11.8	6.0	3.0
59	23327 K	67° 48.3′ N	06° 01.2′ E	1310	11.9	6.1	6.1
60	23239 K	67° 29.8′ N	08° 21.5′ E	1529	12.2	5.6	11.5
61	23054 K	67° 39.4′ N	05° 47.8′ E	1425	11.8	6.1	7.1
62	23069 K	67° 39.9′ N	01° 35.3′ E	1895	11.5	5.9	12.6
63	23074 K	66° 40.2′ N	04° 54.8′ E	1160	12.3	6.1	9.3
64	23072 K	67° 00.1′ N	03° 51.1′ E	1398	12.2	6.2	11.5
65	23071 K	67° 05.1′ N	02° 54.3′ E	1306	11.9	6.3	12.9
66	71-26 B	67° 20.1′ N	02° 09.9′ E	1483	11.5	6.0	7.6
67	23359 K	65° 31.7′ N	04° 08.8′ W	2820	9.7	3.8	4.1
68	71-28 B	65° 40.0′ N	03° 42.5′ W	3140	10.0	4.4	7.6
69	49B-03 B	64° 50.7′ N	01° 31.4′ W	3004	11.2	5.9	8.8
70	49B-04 B	64° 33.9′ N	00° 43.4′ W	2798	11.7	6.3	9.6
71	49B-05 B	64° 26.4′ N	00° 23.7′ W	2702	11.9	6.4	16.8
72	49B-07 B	64° 08.5′ N	00° 23.4′ E	2500	12.1	6.7	11.5
73	49B-08 B	64° 00.7′ N	00° 43.5′ E	2403	12.2	6.8	32.1
74	49B-10 B	63° 50.2′ N	01° 10.6′ E	2200	12.4	7.1	14.5
75	49B-13 B	63° 45.3′ N	01° 23.2′ E	1900	12.6	7.2	22.5
76	49A-11 B	63° 59.3′ N	01° 17.0′ W	2605	11.8	6.3	11.8
77	49B-15 B	63° 09.3′ N	02° 49.6′ E	1002	12.1	6.7	18.5
78	49A-41 B	63° 04.3′ N	03° 20.3′ E	900	12.1	6.1	6.4
79	49B-19 B	62° 46.2′ N	03° 43.1′ E	607	13.4	6.3	22.0
80	49A-04 B	62° 07.4′ N	02° 43.2′ E	410	13.6	5.8	barren
81	49A-06 B	62° 36.9′ N	01° 43.4′ E	702	13.3	6.4	barren
82	49A-07 B	62° 56.6′ N	01° 02.1′ E	1100	12.8	6.9	15.8
83	52-03 B	62° 12.0′ N	00° 00.0′ E	705	12.8	7.2	21.6
84	52-04 B	61° 21.4′ N	03° 21.4′ W	1356	12.4	7.8	14.1
85	52-08 B	60° 06.2′ N	07° 05.1′ W	695	12.6	7.9	34.2
86	52-10 B	59° 58.7′ N	07° 45.3′ W	601	12.6	7.9	barren
87	52-14 B	60° 24.0′ N	12° 25.4′ W	300	12.2	8.3	barren
88	52-15 B	61° 37.9′ N	16° 29.9′ W	2355	12.7	7.9	32.9
89	52-19 B	62° 52.7′ N	15° 09.3′ W	1838	12.0	7.2	16.2
90	52-17 B	62° 20.2′ N	14° 37.0′ W	1800	11.7	7.8	barren
91	52-18 B	62° 27.2′ N	14° 13.8′ W	1672	11.5	7.8	barren
92	52-22 B	63° 11.6′ N	13° 36.0′ W	1102	11.1	7.2	barren
93	52-24 B	63° 21.0′ N	13° 18.8′ W	804	11.1	7.2	barren
94	52-27 B	63° 44.9′ N	12° 33.8′ W	506	10.0	5.8	barren
95	52-28 B	63° 59.7′ N	12° 05.7′ W	406	9.4	5.1	barren
96	49B-01 B	64° 50.9′ N	07° 42.5′ W	2683	8.9	3.1	18.6
97	V30-128 L	64° 04.0′ N	30° 13.0′ W	2310	10.1	4.4	19.2
98	V23-034 L	62° 35.0′ N	26° 57.0′ W	1414	12.1	6.4	19.7
99	V30-126 L	58° 34.0′ N	35° 30.0′ W	2456	10.0	6.1	5.6
100	V30-110 L	57° 22.0′ N	39° 12.0′ W	3256	9.8	5.6	4.4
101	V30-103 L	52° 46.0′ N	36° 35.0′ W	3481	13.9	6.7	26.8
102	V30-177 L	54° 04.0′ N	24° 11.0′ W	3433	14.4	8.9	49.2
103	RC9-228 L	52° 32.9′ N	18° 45.4′ W	3981	15.3	10.2	61.0
104	V23-083 L	49° 52.0′ N	24° 15.0′ W	3871	16.7	10.9	83.0

[a] Sample numbers as listed on Figure 3.
[b] Station number with repository B, Geological Institute B, University of Bergen; K, Sonderforschungsbereich 313, University Kiel; L, Lamont Dohorty Geological Observatory.
[c] Temperatures from Kellogg [1976].
Samples with same August and February temperatures lie under prolonged sea ice cover.
[d] Number of valves per gram dry sediment (in millions).

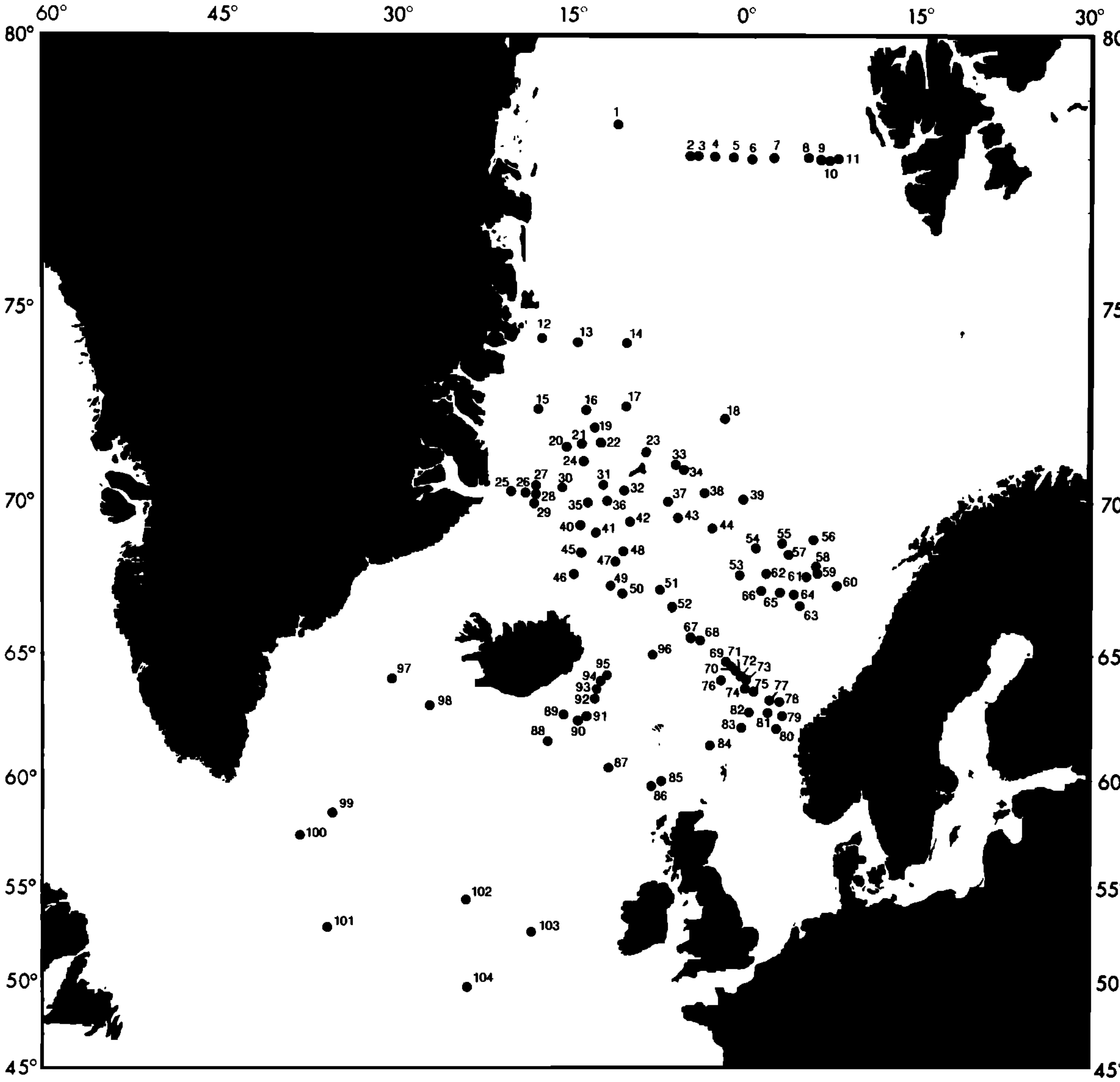

Fig. 2. Location of surface sediment samples used in this study.

TABLE 2. Location and Holocene Sedimentation Rate of the Two Piston Cores

	Position		Water Depth m	Average Sedimentation Rate,[a] cm/1000 yrs	Core Type[b]
	Latitude	Longitude			
Core 57-5	69° 26.0'N	13° 07.0'W	1902	2.1	PC
Core 52-43	64° 31.0'N	00° 44.0'E	2781	4.5	PC

[a] sedimentation rate for the interval Holocene-Present.
[b] PC, piston core.

TABLE 3. Diatom Abundance, B-Hat Matrix, and Estimated Paleotemperatures of Core 57-5

Core 57-5									Estimated SST	
Depth, cm	Abundance (x10^6)	Comunal	Factor 1	Factor 2	Factor 3	Factor 4	Factor 5	Factor 6	August	February
0-2.5	19.48	0.9076	0.1340	0.7668	0.0566	0.5299	0.0489	0.1239	6.8	1.3
2.5-5.0	17.77	0.9321	0.1443	0.8474	0.0586	0.4212	0.0520	0.0983	6.3	0.9
5.0-7.5	19.01	0.8837	0.1274	0.6261	0.0415	0.6864	0.0449	-0.0237	6.9	1.7
7.5-10.0	19.53	0.9051	0.1004	0.5508	0.0391	0.7083	0.2533	-0.1555	8.2	2.7
10.0-12.5	23.49	0.8907	0.1257	0.3856	0.0302	0.6908	0.4909	-0.0845	10.8	5.1
12.5-15.0	20.21	0.8574	0.1136	0.2704	0.0237	0.5432	0.6850	-0.0811	11.6	6.3
15.0-17.5	35.12	0.8532	0.1293	0.1398	0.0150	0.3014	0.8516	-0.0255	12.3	7.6
17.5-20.0	18.91	0.8777	0.1131	0.1860	0.0197	0.5551	0.7132	-0.1143	11.9	6.7
20.0-22.5	14.75	0.8126	0.1050	0.1784	0.0224	0.6147	0.6136	-0.1221	11.1	6.2

TABLE 4. Diatom Abundance, B-Hat Matrix, and Estimated Paleotemperatures of Core 52-43

Core 52-43									Estimated SST	
Depth, cm	Abundance (x10^6)	Comunal	Factor 1	Factor 2	Factor 3	Factor 4	Factor 5	Factor 6	August	February
0-2.5	19.71	0.9388	0.6263	0.3609	-0.0043	0.1876	0.0005	0.6174	10.9	5.7
2.5-5.0	19.85	0.9195	0.5260	0.4292	0.0110	0.1126	0.0347	0.6668	10.1	5.2
5.0-7.5	19.26	0.8189	0.5992	0.3420	0.0020	0.1777	0.0710	0.5534	11.0	5.9
7.5-10.0	21.47	0.9243	0.5827	0.3631	-0.0001	0.2877	0.1188	0.5967	12.0	6.4
10.0-12.5	20.31	0.8618	0.6471	0.3238	0.0112	0.2834	0.2780	0.4247	13.4	7.2
12.5-15.0	18.59	0.8821	0.6756	0.2807	0.0066	0.1675	0.3415	0.4495	13.7	7.8
15.0-17.5	17.16	0.9060	0.4523	0.1613	0.0151	0.1638	0.7883	0.1639	14.7	9.0
17.5-20.0	19.20	0.8798	0.2582	0.0434	0.0103	0.1190	0.8909	0.0562	13.2	8.7
20.0-22.5	18.16	0.9001	0.3094	0.0205	0.0116	0.1148	0.8878	0.0495	13.6	9.0
22.5-25.0	23.06	0.8979	0.2658	0.0152	0.0095	0.1076	0.9011	0.0582	13.3	8.9
25.0-27.5	19.49	0.8735	0.2023	0.0062	0.0094	0.1134	0.9042	0.0448	12.8	8.6
27.5-30.0	16.74	0.8720	0.1933	-0.0010	0.0075	0.0887	0.9076	0.0540	12.6	8.6
30.0-32.5	24.13	0.8685	0.1480	-0.0093	0.0083	0.1121	0.9131	0.0124	12.2	8.4
32.5-35.0	25.76	0.8651	0.1452	-0.0095	0.0069	0.1177	0.9107	0.0258	12.3	8.4
35.0-37.5	23.02	0.8641	0.1434	-0.0054	0.0068	0.1057	0.9115	0.0379	12.2	8.4
37.5-40.0	24.12	0.8610	0.1319	-0.0123	0.0074	0.1096	0.9115	0.0215	12.1	8.3
40.0-42.5	25.86	0.8646	0.1318	-0.0117	0.0072	0.1253	0.9116	0.0156	12.1	8.3
42.5-45.0	18.48	0.8755	0.1585	-0.0011	0.0080	0.1157	0.9143	0.0321	12.4	8.5
45.0-47.5	8.87	0.8561	0.1437	-0.0155	0.0074	0.1019	0.9076	0.0307	12.2	8.4
47.5-50.0	1.47	0.8136	0.1743	-0.0005	0.0118	0.0917	0.8798	0.0236	12.1	8.2

TABLE 5. Varimax Factor Matrix From Q Mode Factor Analysis of Surface Sediment Samples

Station	Communality	Factor 1	Factor 2	Factor 3	Factor 4	Factor 5	Factor 6
71-12	0.979	0.132	0.923	0.064	0.226	0.023	0.168
71-17	0.992	0.093	0.977	0.084	0.126	0.009	0.011
71-21	0.962	0.257	0.856	0.064	0.341	0.014	0.192
71-26	0.913	0.934	0.079	0.025	0.082	-0.055	0.138
71-19	0.962	0.164	0.803	0.048	0.487	0.008	0.101
71-20	0.984	0.142	0.956	0.082	0.025	0.010	0.152
71-25	0.975	0.745	0.316	0.014	0.356	-0.073	0.432
71-22	0.936	0.397	0.451	0.033	0.719	-0.117	0.142
71-14	0.928	0.006	0.839	0.109	-0.158	0.060	-0.301
71-28	0.982	0.389	0.455	-0.001	0.441	-0.026	0.654
57-14	0.976	0.397	0.611	0.030	0.457	-0.048	0.482
57-12	0.934	0.396	0.636	0.047	0.556	0.022	0.015
57-10	0.807	0.152	0.715	0.076	0.314	-0.024	0.055
57-09	0.914	0.131	0.864	0.095	0.288	0.010	0.006
57-08	0.956	0.150	0.712	0.047	0.477	0.053	0.177
57-06	0.948	0.107	0.943	0.065	0.162	0.025	0.089
57-05	0.973	0.124	0.607	0.014	0.676	-0.029	0.214
57-04	0.945	0.152	0.652	0.029	0.607	0.000	0.141
52-03	0.930	0.948	0.089	0.022	0.122	0.045	-0.035
52-04	0.919	0.845	0.249	0.029	0.259	0.165	0.214
52-08	0.977	0.868	0.063	0.018	0.064	0.450	0.048
52-15	0.939	0.785	0.037	0.032	0.292	0.439	0.018
52-19	0.943	0.838	0.045	0.032	0.115	0.467	-0.073
49A-07	0.978	0.936	0.170	0.044	0.002	0.216	-0.130
49A-11	0.979	0.595	0.462	0.015	0.161	0.064	0.617
49A-41	0.874	0.895	0.156	0.084	-0.050	0.046	-0.170
49B-01	0.948	0.220	0.602	0.041	0.668	0.043	0.200
49B-03	0.990	0.444	0.428	-0.004	0.168	0.000	0.761
49B-04	0.940	0.616	0.444	0.014	0.156	0.135	0.553
49B-05	0.968	0.848	0.293	0.023	0.156	0.112	0.303
49B-07	0.969	0.623	0.512	0.021	0.129	0.234	0.492
49B-08	0.950	0.625	0.438	0.022	0.432	0.053	0.401
49B-10	0.942	0.718	0.164	0.022	0.065	0.607	0.115
49B-13	0.980	0.752	0.316	0.018	0.218	0.372	0.336
49B-15	0.898	0.919	0.040	0.029	-0.026	0.029	-0.141
49B-19	0.928	0.929	-0.012	0.023	0.136	0.181	-0.109
21291	0.950	0.059	0.225	0.932	0.095	-0.024	0.060
21292	0.878	0.014	0.131	0.904	0.061	-0.008	0.039
21293	0.937	0.034	0.207	0.937	0.045	-0.004	-0.011
21294	0.936	0.053	0.357	0.851	0.049	0.000	0.055
21295	0.978	0.060	0.667	0.538	0.038	0.025	0.033
21296	0.980	0.047	0.626	0.602	-0.038	0.033	0.011
21297	0.964	0.054	0.677	0.669	-0.085	0.033	-0.048
21298	0.981	0.012	0.235	0.958	-0.022	0.004	0.039
21302	0.983	0.000	0.203	0.944	-0.037	-0.001	-0.010
23239	0.923	0.940	0.057	0.020	0.143	0.057	0.094
23054	0.980	0.971	0.069	0.053	0.128	0.006	0.112
23055	0.952	0.784	0.345	0.038	0.245	0.022	0.394
23056	0.966	0.740	0.369	0.040	0.419	-0.075	0.313
23059	0.959	0.278	0.331	0.014	0.862	-0.071	0.069
23065	0.960	0.593	0.363	0.026	0.483	-0.117	0.391
23069	0.984	0.892	0.233	0.023	0.223	-0.006	0.288
23071	0.955	0.969	0.017	0.021	0.040	0.072	0.072
23072	0.916	0.941	0.014	0.027	0.111	-0.002	0.096
23074	0.969	0.976	0.046	0.026	0.079	0.061	0.045
23327	0.968	0.915	0.005	0.027	0.212	-0.027	0.095

TABLE 5. (continued)

Station	Communality	Factor 1	Factor 2	Factor 3	Factor 4	Factor 5	Factor 6
23334	0.976	0.528	0.624	0.071	0.332	0.020	0.293
23335	0.968	0.975	0.048	0.023	0.081	-0.050	0.041
23337	0.976	0.501	0.354	0.130	0.590	-0.065	0.266
23338	0.943	0.111	0.691	0.587	0.162	0.000	0.035
23341	0.995	0.166	0.910	0.104	0.047	0.012	0.343
23342	0.985	0.106	0.934	0.263	0.134	0.001	0.046
23343	0.969	0.053	0.824	0.448	-0.042	0.039	-0.229
23345	0.992	0.087	0.935	0.285	0.124	0.013	-0.010
23346	0.992	0.118	0.935	0.138	0.274	-0.013	0.075
23347	0.990	0.065	0.849	0.443	0.217	0.002	-0.112
23348	0.953	-0.021	-0.060	0.961	0.009	-0.005	0.054
23349	0.965	-0.019	-0.005	0.968	-0.003	-0.004	0.023
23350	0.957	-0.021	-0.034	0.964	0.003	-0.004	0.041
23351	0.956	0.003	0.139	0.956	0.030	-0.003	-0.003
23352	0.993	0.150	0.921	0.070	0.173	0.000	0.294
23353	0.997	0.121	0.964	0.083	0.065	0.014	0.181
23354	0.996	0.129	0.957	0.080	0.161	0.000	0.163
23359	0.970	0.343	0.495	0.017	0.608	-0.054	0.479
23295	0.970	0.137	0.878	0.279	0.305	-0.018	0.037
ArkV-147	0.843	0.013	0.638	0.451	-0.077	0.062	-0.097
V30-103	0.954	0.263	0.036	0.022	0.776	0.339	0.046
V30-177	0.905	0.295	-0.026	0.011	0.200	0.874	0.027
V30-110	0.964	0.209	0.191	0.019	0.932	0.062	-0.023
V30-128	0.952	0.184	0.231	0.030	0.903	0.190	0.082
V30-130	0.815	0.353	0.130	0.789	0.050	-0.001	-0.097
V30-126	0.989	0.190	0.187	0.009	0.942	0.176	0.003
V23-034	0.958	0.332	0.297	0.008	0.551	0.423	0.492
V23-083	0.971	0.307	-0.030	0.009	0.061	0.934	0.011
RC9-228	0.864	0.597	-0.035	0.012	-0.012	0.703	-0.012
Variance		27.018	28.265	14.608	11.738	4.498	5.610
Cumulative variance		27.018	55.283	69.892	81.629	86.127	91.738

For core locations see Table 1.

were barren of diatoms. The barren samples were located where the Upper Norwegian Deep Water [Hopkins, 1988] overflows to the North Atlantic along the eastern Iceland slope and south of the Færoe Islands or at the Greenland continental slope where currents flow parallel to the continental slope. The fact that these samples underlie intermediate current pathways might reflect winnowing and dissolution rather than a lack of opal production in the overlying water masses.

Q mode factor analysis applied to 43 diatom species and species groups from 87 surface sediment samples on a *Chaetoceros* free basis (see Schrader and Koc Karpuz [1990] for discussion) allowed the definition of six significantly different floral assemblages which explained 91.7% of the total variance (Table 5). The factor compositions are tabulated in Table 6. The communalities are generally higher than 0.80 (sample 57-10) in all samples (Table 5). Mapping of the six factors (Figures 3a-3f; contouring of varimax matrix values *100 was done at >70, 70-20, and <20 intervals and at other intervals in Figures 3b, 3d, and 3f) showed their close affinity to hydrographic regimes of the GIN Sea. These are the Norwegian-Atlantic Current (NAC) assemblage, Arctic Water (AW) assemblage, Sea Ice (SI) assemblage, Arctic-Norwegian Waters Mixing (ANWM) assemblage, Atlantic (A) assemblage, Norwegian-Arctic Waters Mixing (NAWM) assemblage.

Factor 1 (Figure 3a). The Norwegian-Atlantic Current assemblage consists primarily of *Thalassionema nitzschioides, Paralia sulcata*, and *Proboscia alata* [Sundström, 1986] (synonym for *Rhizosolenia alata*)(in the order of importance). Highest loadings of this factor occur in sediments underlying the Norwegian-Atlantic Current (Figure 4), with successively decreasing loadings toward the west. Both *Thalassionema nitzschioides* and *Paralia sulcata* are cosmopolitan species; in the GIN Sea they are

TABLE 6. Varimax Factor Score Matrix From Factor Analysis of Surface Sediment Samples

Variable	Factor 1	Factor 2	Factor 3	Factor 4	Factor 5	Factor 6
Thalassiothrix longissima	0.031	0.021	-0.002	0.148	0.053	0.070
Thalassionema nitzschioides	0.684	-0.051	0.005	-0.117	0.141	-0.010
Rhizosolenia hebetata f.heb.	-0.001	0.099	-0.019	0.042	0.006	-0.012
Rhizosolenia hebetata f.semi.	0.021	0.179	0.001	0.874	-0.062	-0.203
Rhizosolenia borealis	0.202	-0.101	0.024	0.388	-0.015	0.139
Proboscia alata	0.323	-0.052	-0.002	0.042	-0.191	0.055
Rhizosolenia bergonii	-0.001	0.000	0.000	-0.001	0.031	0.000
Bacterosira fragilis	-0.001	0.017	0.050	-0.004	0.006	-0.014
Biddulphia aurita	0.003	-0.002	0.008	-0.001	0.000	-0.002
Paralia sulcata	0.532	-0.011	0.021	-0.083	-0.147	-0.306
Roperia tesselata	0.052	-0.006	0.000	-0.005	0.065	-0.017
Porosira glacialis	0.004	0.007	0.033	-0.004	0.000	-0.006
Actinocyclus curvatulus	0.030	0.076	0.019	0.012	0.037	-0.023
Asteromphalus robustus	0.002	0.015	0.000	0.008	0.006	0.010
Hemidiscus cuneiformis	-0.003	0.000	0.000	-0.002	0.037	0.001
Thalassiosira gravida spore	0.007	0.744	0.094	-0.148	0.029	-0.364
Thalassiosira gravida veg.	0.166	0.485	-0.017	0.021	-0.034	0.810
Thalassiosira leptopus	-0.026	0.356	0.033	-0.075	0.064	-0.180
Thalassiosira eccentrica	0.088	-0.004	-0.001	-0.022	0.023	-0.023
Thalassiosira trifulta	0.007	0.101	0.019	-0.007	0.012	-0.015
Thalassiosira lineata	0.027	-0.003	0.000	-0.021	0.008	0.062
Thalassiosira nordenskioeldii	0.075	0.026	0.062	0.042	-0.057	-0.024
Thalassiosira oestrupii	0.085	-0.032	0.007	0.077	0.915	0.006
Thalassiosira hyalina	-0.002	0.024	0.131	-0.011	-0.001	0.008
Thalassiosira angulata	0.158	-0.017	0.004	-0.025	-0.107	-0.050
Thalassiosira pacifica	0.061	-0.010	0.017	-0.004	-0.028	-0.030
Thalassiosira ferelineata	0.014	-0.002	0.002	-0.001	0.004	-0.012
Thalassiosira decipiens	0.004	-0.001	0.000	-0.001	0.011	-0.003
Coscinodiscus radiatus	0.136	-0.017	-0.002	0.008	-0.088	0.030
Coscinodiscus marginatus	0.001	-0.001	0.000	0.004	0.002	0.002
Coscinodiscus nodulifer	0.000	0.000	0.000	-0.001	0.010	0.000
Coscinodiscus oculus-iridis	0.009	-0.001	0.001	0.009	-0.012	0.009
Coscinodiscus asteromphalus	0.014	-0.004	0.000	0.007	-0.012	0.009
Nitzschia marina	-0.004	-0.009	0.002	0.037	0.076	-0.003
Nitzschia bicapitata	0.019	-0.007	0.000	0.007	0.177	-0.022
Nitzschia cylindra	-0.009	-0.024	0.207	-0.007	-0.002	0.038
Nitzschia angularis	0.003	0.001	0.006	0.009	-0.001	0.012
Nitzschia grunowii	-0.022	-0.076	0.959	0.011	-0.006	0.055
Bacteriastrum hyalinum	0.001	-0.001	0.000	0.000	0.031	0.004
Melosira ambigua	0.014	-0.001	0.003	-0.003	-0.007	-0.005
Pleurosigma spp.	0.010	0.000	0.000	-0.001	0.001	-0.006
Synedra spp.	0.007	-0.007	0.004	0.022	0.034	-0.017
Navicula spp.	-0.002	0.016	0.023	-0.007	0.002	-0.006

associated with the Atlantic waters (salinities >34.9‰ and SST >3°C). *Paralia sulcata* is also a neritic species and is commonly found in near-continental marine sediments [Hustedt, 1930, 1959]. Here it is confined to the continental margins of Norway and southern Iceland.

Factor 2 (Figure 3b). The Arctic Water assemblage consists mainly of *Thalassiosira gravida* spores together with *Thalassiosira gravida* vegetative cells and *Thalassiosira leptopus* as secondary components. It has its highest loadings in waters between the Polar and the Atlantic waters, i.e., the Arctic waters with salinities between 34.7 to 34.9‰ and temperatures ranging from freezing to 8°C. *Thalassiosira gravida* spores have been frequently reported from high-latitude areas which are seasonally sea ice covered [Ramsfjell, 1960; Kanaya and Koizumi, 1966; Jousé et al., 1971; Sancetta, 1982; Williams, 1986].

Factor 3 (Figure 3c). The Sea Ice assemblage consists of *Nitzschia grunowii* and *Nitzschia cylindra* and to a lesser degree of *Thalassiosira hyalina*, *Thalassiosira gravida* spores, *Bacterosira fragilis*, and *Porosira glacialis*. The

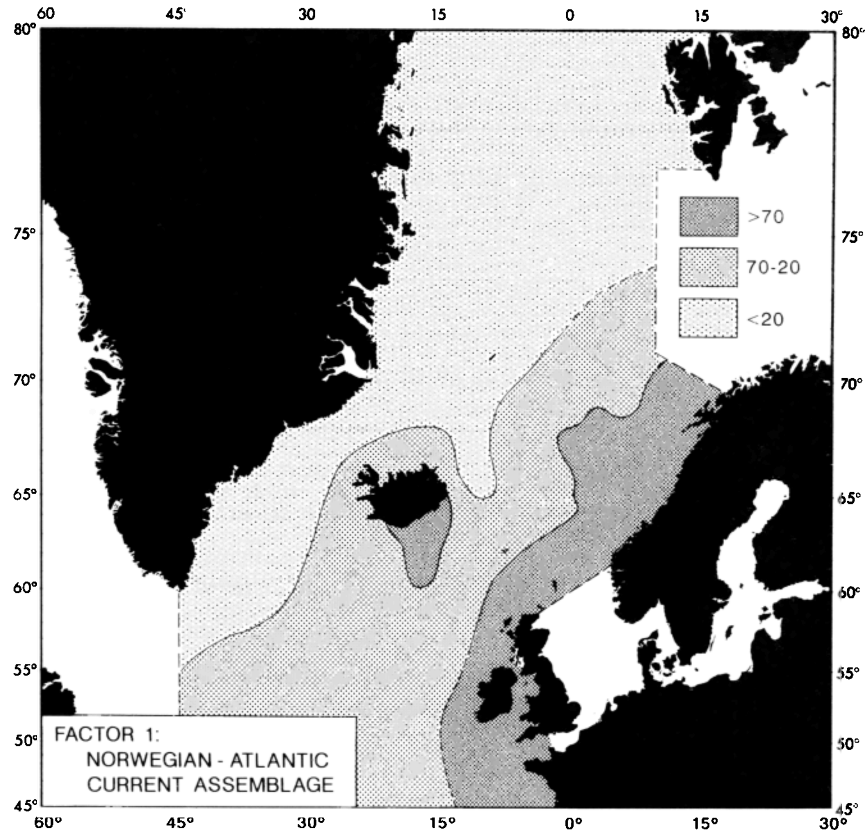

Fig. 3a. Geographic distribution of factor 1. Values plotted are those from varimax matrix *100.

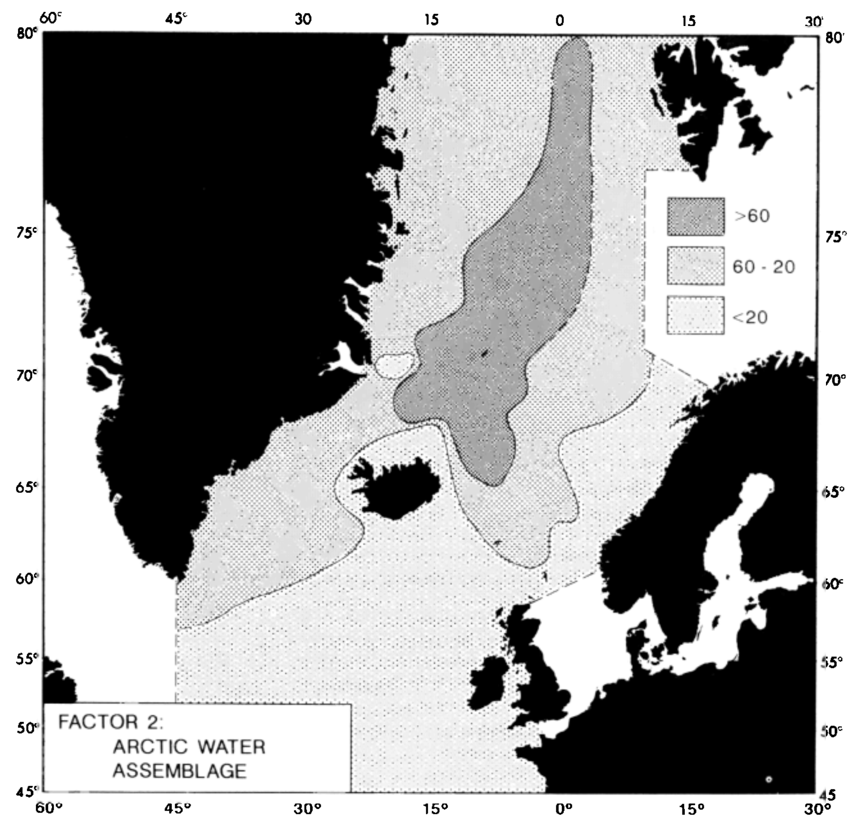

Fig. 3b. Same as Figure 3a, except for factor 2.

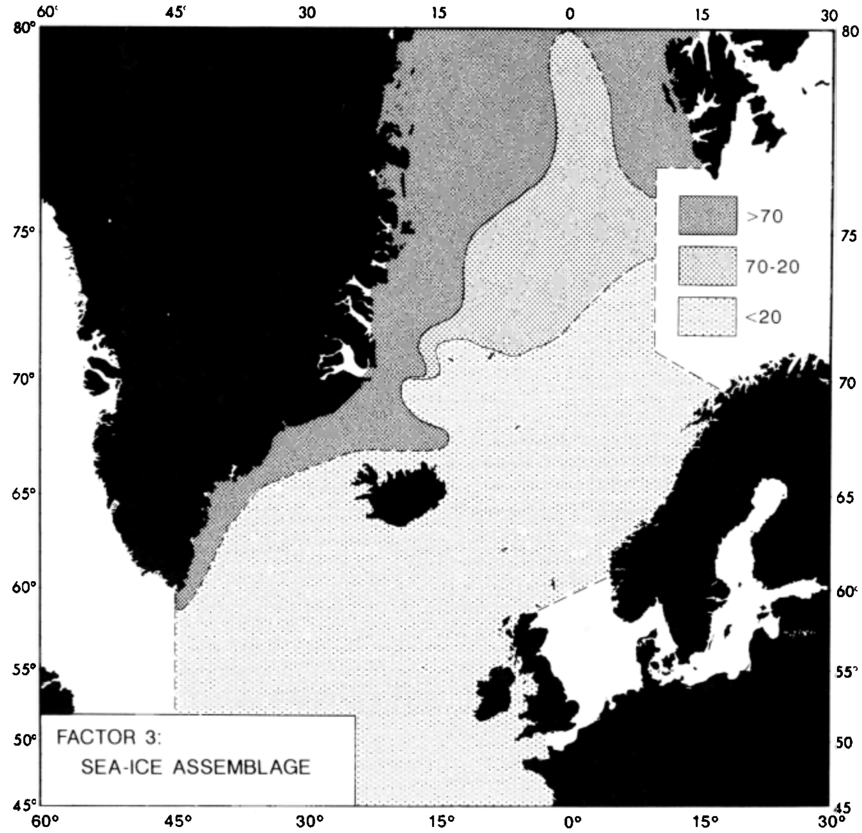

Fig. 3c. Same as Figure 3a, except for factor 3.

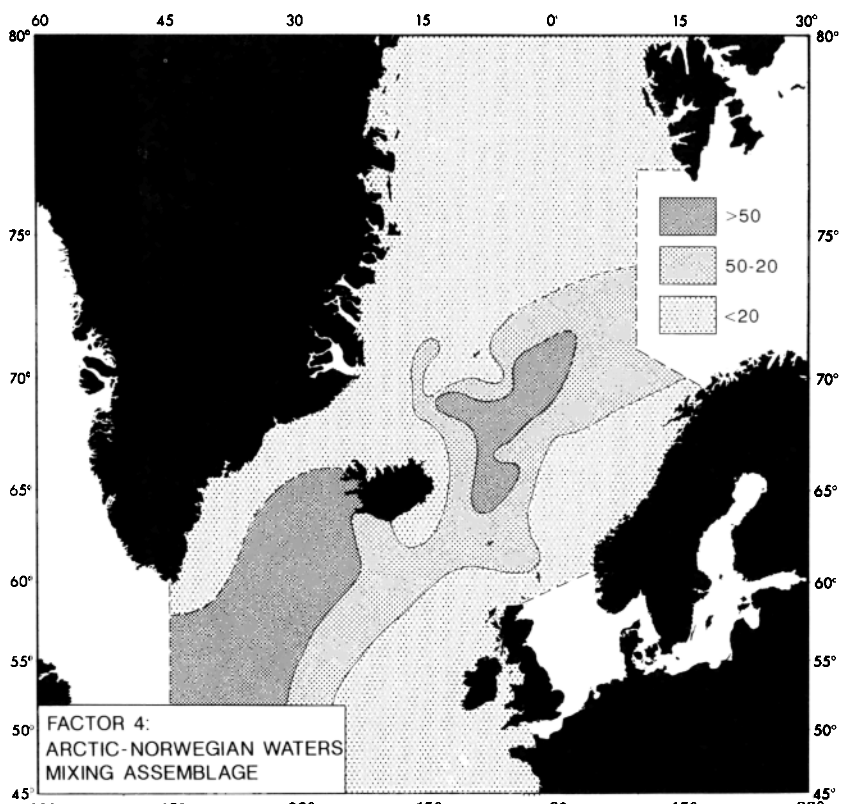

Fig. 3d. Same as Figure 3a, except for factor 4.

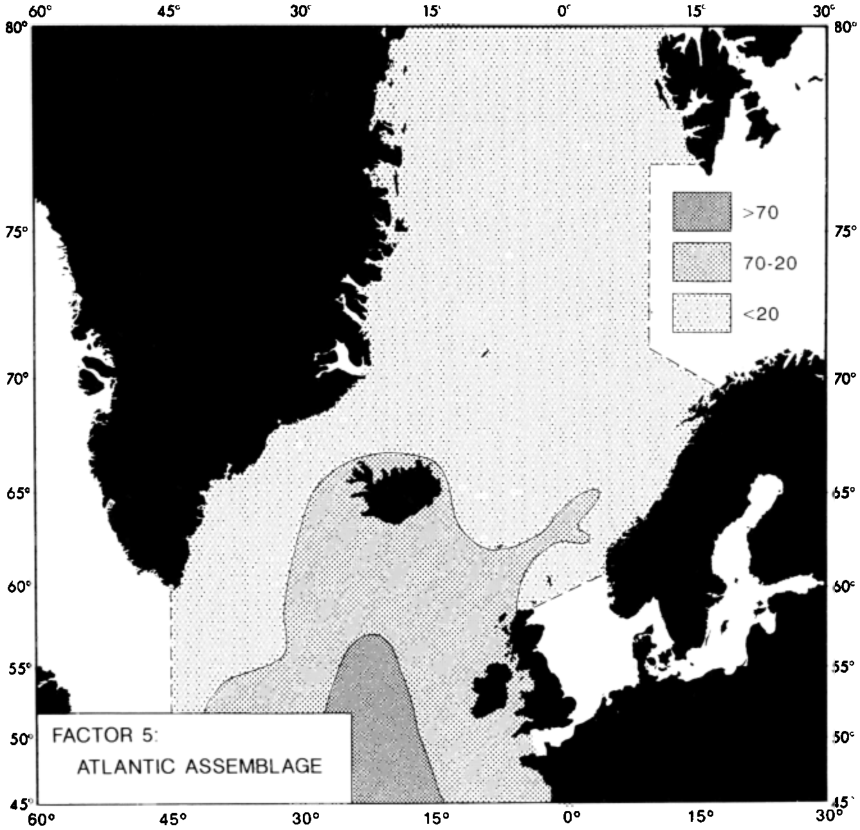

Fig. 3e. Same as Figure 3a, except for factor 5.

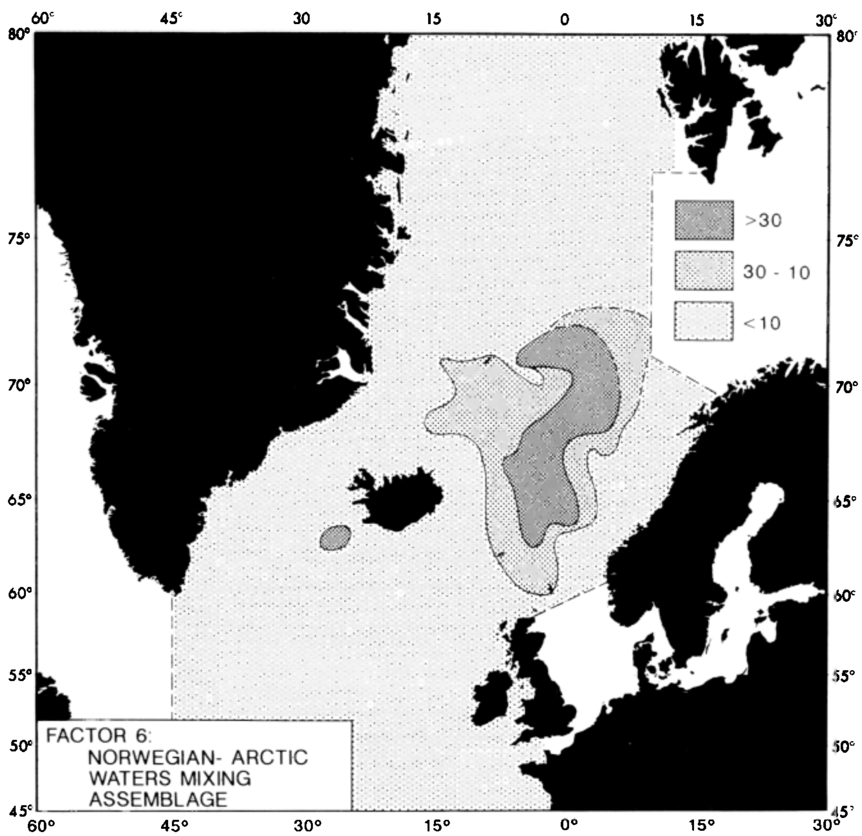

Fig. 3f. Same as Figure 3a, except for factor 6.

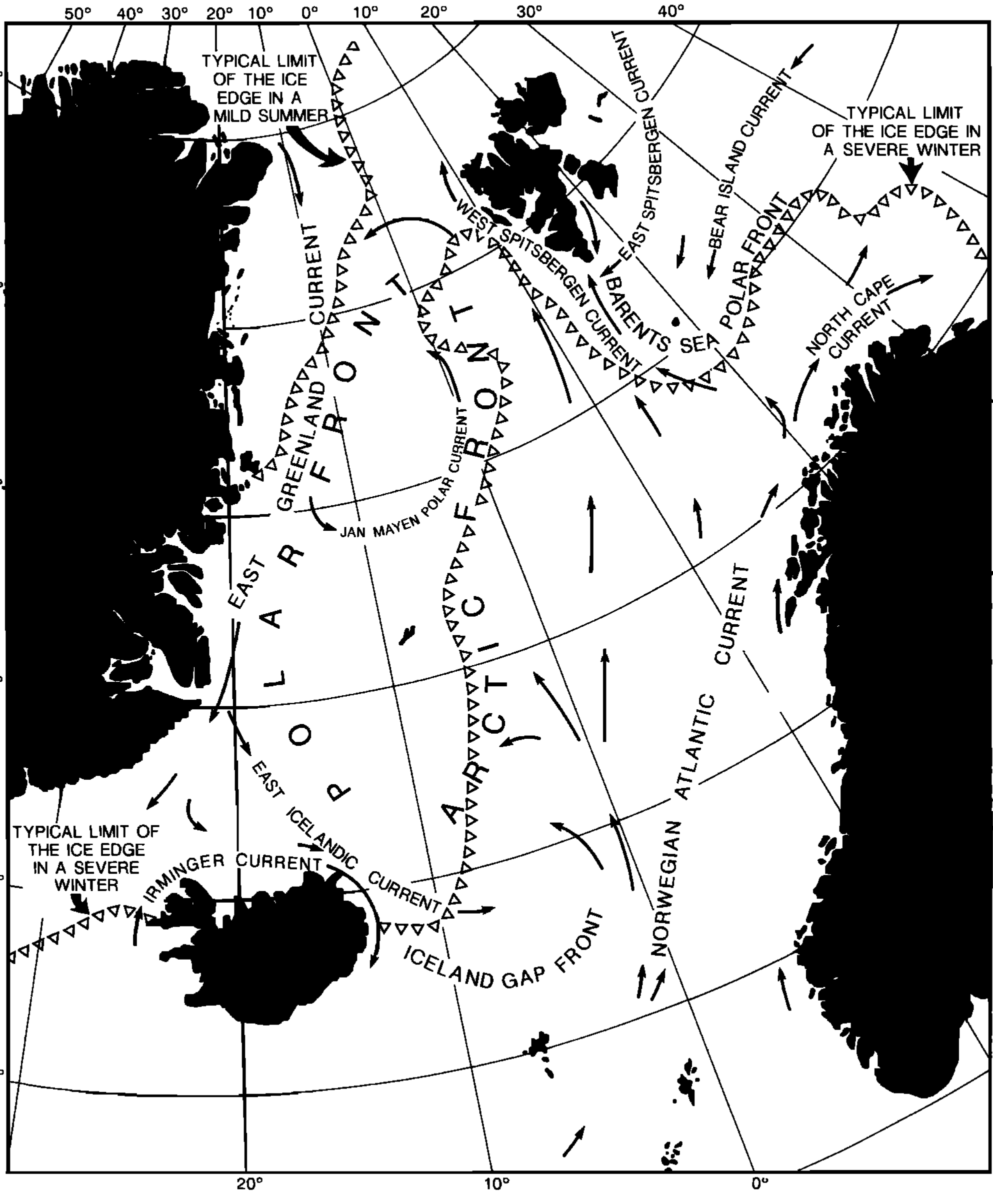

Fig. 4. Major currents and sea ice features in the Nordic Seas [from Hurdle, 1986].

distribution of this assemblage shows a close relation to the spring sea ice limit of the GIN Sea (Figure 4). Species of this assemblage have often been reported from ice packs, ice margin plankton collections, and high-latitude sediments underlying such areas [Horner, 1982; Sancetta, 1982; Horner, 1985; Williams, 1986]. Horner [1982] reports that while the ice algal bloom consists primarily of pennate diatoms, the phytoplankton bloom at the ice edge consists mainly of centric diatoms and that *Nitzschia grunowii* and *Nitzschia cylindra* are abundant in both habitats. *Thalassiossira hyalina* is also an Arctic species which in the GIN Sea is confined to the western part where it is a component of the "drift ice flora" [Smayda, 1957]. Grant and Horner [1976] characterize *Porosira glacialis* as a common constituent of the Arctic phytoplankton especially during the spring bloom, but add that it is not unusual to find it in sea ice.

Factor 4 (Figure 3d). The Arctic-Norwegian Waters Mixing assemblage consists mainly of *Rhizosolenia hebetata* f. *semispina* and *Rhizosolenia borealis* [Sundström, 1986] (synonym for *Rhizosolenia styliformis*) and to a lesser degree of *Thalassiothrix longissima*. It has its highest loadings in areas of mixture between the Arctic and the Atlantic waters (Figure 1), northeast and southwest of Iceland. Gran [1904] and Paasche [1960] had reported the maximum abundance of *Rhizosolenia hebetata* f. *semispina* in the GIN Sea in an area between the Arctic and Atlantic water masses. Smayda [1957] observed active growth of this species around Jan Mayen at suface water temperatures of 1.5°C and concluded that it forms the principal constituent of the summer Arctic phytoplankton community.

Factor 5 (Figure 3e). The Atlantic assemblage consists mainly of *Thalassiosira oestrupii*. The highest loadings of this factor occur in the North Atlantic, under the warm North Atlantic water mass (Figure 1) (salinities >35.3‰, SST >8°C). Maynard [1976] also reports *Thalassiosira oestrupii* as the main component of her factor 5 (Subtropical assemblage), in the North Atlantic. Mapping of the relative abundance of *Globigerina bulloides* [Kipp, 1976] and factor 2 (equation 2) of Kellogg [1975] in the North Atlantic also shows a similar distribution to factor 5.

Factor 6 (Figure 3f). The Norwegian-Arctic Waters Mixing assemblage consists mainly of *Thalassiosira gravida* vegetative cells. It has its highest loadings in an intermediate area between the Atlantic and the Arctic water masses. This factor shows strong similarity in distribution to Kellogg's [1975] factor 3 (equation 1) which consists almost entirely of *G. quinqueloba*.

Transfer functions (GINT2) relating factor distributions to winter (February) and summer (August) surface water temperatures [from Kellogg, 1976] were generated. Factor loadings of the six factors display a uniform succession between -1.7° and 10.9°C for February and between -1.7° and 16.7°C for August. The transfer functions have a standard error of estimate of ±1.5°C (August) and ±1.0°C (February) and have a multiple correlation coefficient (adjusted for degrees of freedom) of 0.942 (August) and 0.964 (February) (Table 7). Plotting observed versus predicted August (Figure 5a) and February (Figure 5b) sea surface temperatures displays a homogeneous scatter over all temperature ranges. Residuals are mostly randomly scattered and show no clustering, except for those samples lying under the winter sea ice cover with -1.7°C.

The Holocene

Downcore studies of core 52-43 from the Norwegian Basin and core 57-5 from the Iceland Plateau (Figure 8) revealed the diatom abundance, assemblage succession and paleotemperature trends (Tables 3 and 4) in the area during the Holocene.

Both cores show high diatom abundance throughout the Holocene, indicating favorable conditions for diatom production in the surface waters and preservation in the sediments. In core 57-5, diatoms are present starting at 20-22.5 cm depth within the Saksunarvatn ash layer (9100 years B.P.)(Figure 6). Diatom abundance increases steadily from there on to a maximum of 35 million valves per gram dry sediment at around 15-17.5 cm depth. Abundance decreases to 20 million valves per gram dry sediment thereafter to the Recent. Diatoms are present in core 52-43 starting within the Vedde ash layer at 50-47.5 cm depth (Figure 7). Diatom abundance increases steadily between 50-42.5 cm to ca 25 million valves per gram dry sediment. A decrease to 17 million valves per gram around 30 cm depth is succeeded by values around 20 million valves per gram up to the Recent without significant variation.

The Holocene diatom data from the cores are described in terms of the surface sediment assemblages. Both cores show significant fluctuations in floral composition; the contributing assemblages range from temperate to polar. Today core 57-5 lies in an area which is characterized primarily by factor 2, AW assemblage, and secondarily by factor 4, ANWM assemblage, whereas core 52-43 is influenced primarily by factor 1, NAC assemblage, and factor 6, NAWM assemblage (Figure 8).

Core 57-5 (Iceland Sea)

The earliest Holocene diatom data from core 57-5 indicates the presence of the ANWM and Atlantic assemblages over the Iceland Plateau (Figure 9). At present, these two assemblages co-occur south of Iceland around 50°-60°N. The same sample also contains some sea ice indicative species. The presence of these sea ice related species exclusively in the lowermost sample might indicate a rapid westward migration of the Polar Front from the area during the late pre-Boreal. The Atlantic assemblage dominated the overlying waters as the ANWM assemblage decreased in importance between 22.5 and 12.5 cm, marking the presence of temperate North Atlantic waters

TABLE 7. Statistical Data for the Transfer Functions and the Regression Coefficients

	August SST	February SST
Multiple correlation coefficient[a]	0.942	0.964
Standard error of estimate[a]	1.503	1.008
Factor 1	9.13863	4.69613
Factor 2	-	-3.41847
Factor 3	-	-2.39075
Factor 4	4.64270	1.90892
Factor 5	8.80125	6.15010
Factor 6	3.32774	3.00677
Intercept	2.27785	1.78802

[a] Adjusted for degrees of freedom.

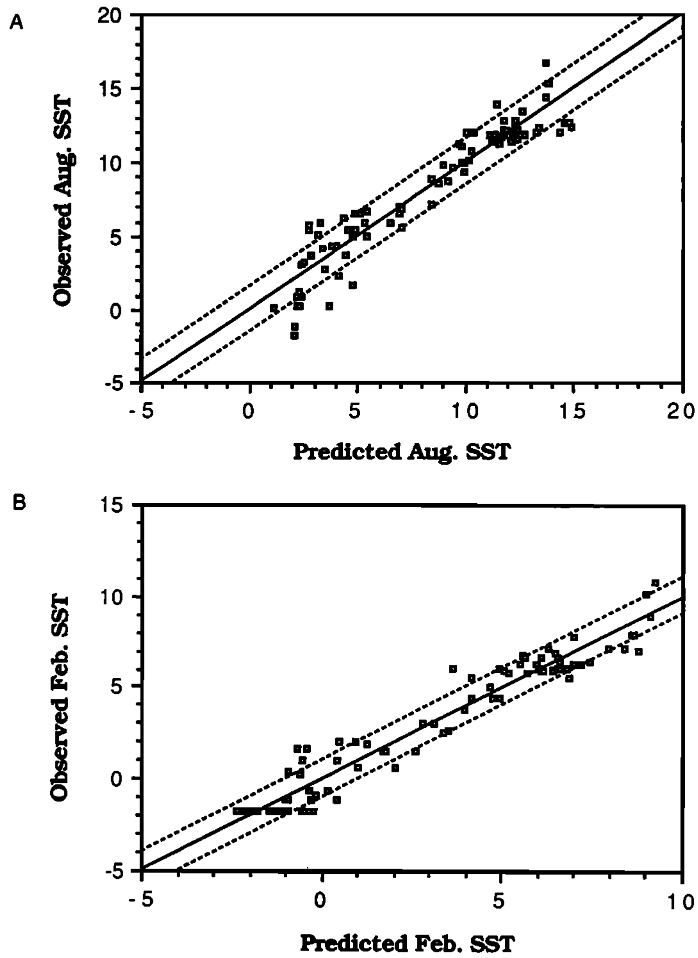

Fig. 5. Observed versus predicted (a) August and (b) February sea surface temperatures.

over the Iceland Plateau. As the contribution of the Atlantic assemblage steadily decreased, contributions of the ANWM and the AW assemblages increased. The ANWM assemblage dominated the depth interval 12.5-5 cm, whereas the AW assemblage dominated from there on to the present. A distinct pattern is observed in which the diatom assemblages first migrated northward as the Atlantic assemblage took over the possibly ice-laden polar and then the Arctic waters. Later, the Atlantic assemblage retreated southwards and the surface waters of the Iceland Sea was replaced by the successive Arctic water assemblages.

Application of the temperature transfer functions (GINT2) to the Holocene diatom assemblage succession from the Iceland Plateau revealed the following paleotemperature trends: (1) higher than present winter and summer SST of 12° and 7°C (August and February, respectively) during the Boreal-Atlantic chronozones (Figure 10), (2) a steady decrease during the Sub Boreal chronozone, and (3) thereafter a slight temperature increase toward the present is observed.

These assemblage succession and paleotemperature trends indicate a strong influx of Atlantic waters onto the Iceland Plateau during the Boreal-Atlantic chronozones. As the influx of the warm Atlantic waters diminished and the Arctic waters dominated the area the sea surface temperatures dropped steadily from the sub-Boreal to the present. The slight temperature increase (0.5°C) at the topmost sample is attributed to the increase in the contribution of the ANWM assemblage which might imply an increase in the westward contribution of the Atlantic waters from the Norwegian-Atlantic current.

Core 52-43 (Norwegian Sea)

Diatoms are present from the middle of Younger Dryas time to the present in core 52-43 (Figure 7). The interval between 50 cm and 15 cm is dominated by the Atlantic assemblage (Figure 11). As the contribution of this assemblage diminishes at 15 cm contributions of the NAC and the NAWM assemblages increase. The NAC assemblage dominates between 15-10 cm. The topmost (0-

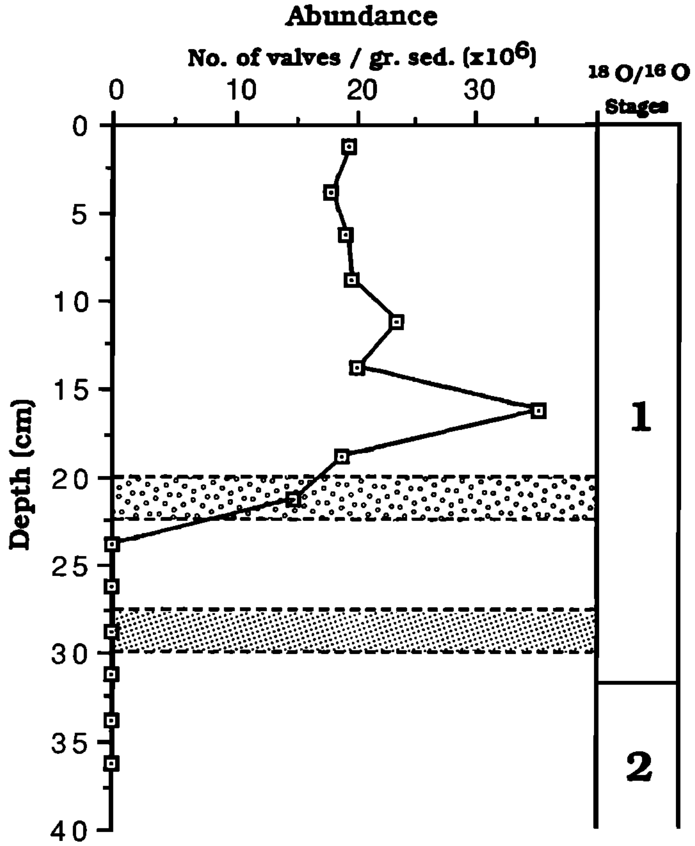

Fig. 6. Downcore Holocene diatom valve abundance plotted against depth and oxygen isotope stages in core 57-5 from the Iceland Plateau. Plotted depths are midpoints of the channel samples. Shaded areas represent the depth intervals of the Vedde ash layer (10,600 years B.P.)(dots) and the Saksunarvatn ash layer (9100 years B.P.)(open circles). Isotope stages from Beyer [1988].

10 cm) part of the core registers alternation of the NAC and the NAWM assemblages over the area.

Application of the temperature transfer functions (GINT2) to the Holocene diatom assemblage succession from the Norwegian Basin revealed the following paleotemperature trends: (1) higher than present winter and summer SST of 12°-14°C and 8°-9°C (August and February, respectively) during the mid-Younger Dryas-mid-sub-Boreal chronozones, with a slight increase in the latter part (Figure 10), (2) a gradual decrease throughout the Sub Atlantic chronozone, and (3) a slight increase to the Present values.

The assemblage successions and paleotemperature estimates of core 52-43 demonstrate the strong contribution of the Atlantic waters beginning from mid-Younger Dryas time and getting reduced in late sub-Boreal time. The modern condition is reached after a period with the dominance of the NAC assemblage, again indicating a significant geographic diatom assemblage migration.

In general, both the Iceland and the Norwegian Seas experienced a strong influx of temperate Atlantic surface waters during the first half of the Holocene, and beginning in the sub-Boreal interval a gradual decrease in SST with a slight increase to the present values is observed. Even though the general trends of the two cores are similar, there are significant differences when it comes to start and duration of the strong influx of the Atlantic waters (the temperature maximum) and the degree of SST difference experienced throughout the time interval in question.

The first occurrence of diatoms in the Norwegian Sea core takes place within the Vedde ash layer, i.e., 10,600 years B.P. However, significant numbers in abundance are not reached til about 10,000 years B.P. Diatoms are first observed within the Saksunarvatn ash layer, i.e., 9100 years B.P. in the Iceland Sea core. In this respect, the postglacial warming of the GIN Sea was time transgressive from east to west.

The strong influx of Atlantic waters over the Iceland Plateau lasted up to the sub-Boreal chronozone. The effect of the temperate Atlantic waters at the core 52-43 location seems to be very stable (Figure 10). A decrease from late sub-Boreal onward implies a longer duration of the strong Atlantic water pulse in the Norwegian Sea compared to the Iceland Sea.

Core 57-5 shows a downcore August and February temperature difference (maximum-minimum) of 5.9° and

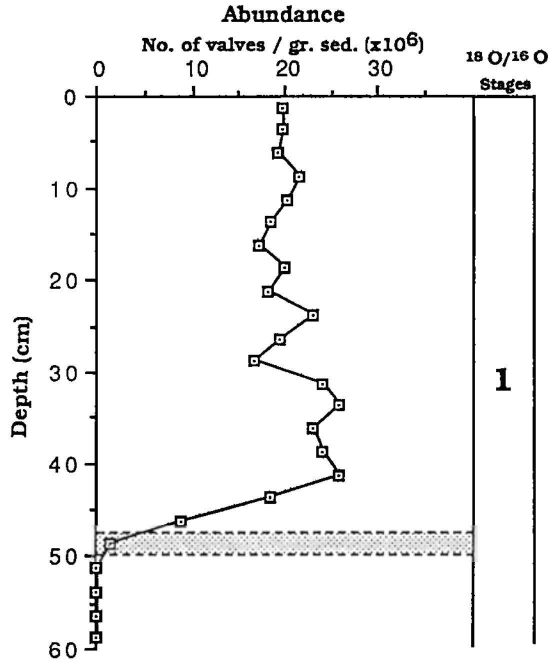

Fig. 7. Downcore Holocene diatom valve abundance plotted against depth and oxygen isotope stages in core 52-43 from the Norwegian Basin. Plotted depths are midpoints of the channel samples. Shaded area represents the depth interval of the Vedde ash layer (10,600 years B.P.). Isotope stages from T. Veum (manuscript in preparation, 1990).

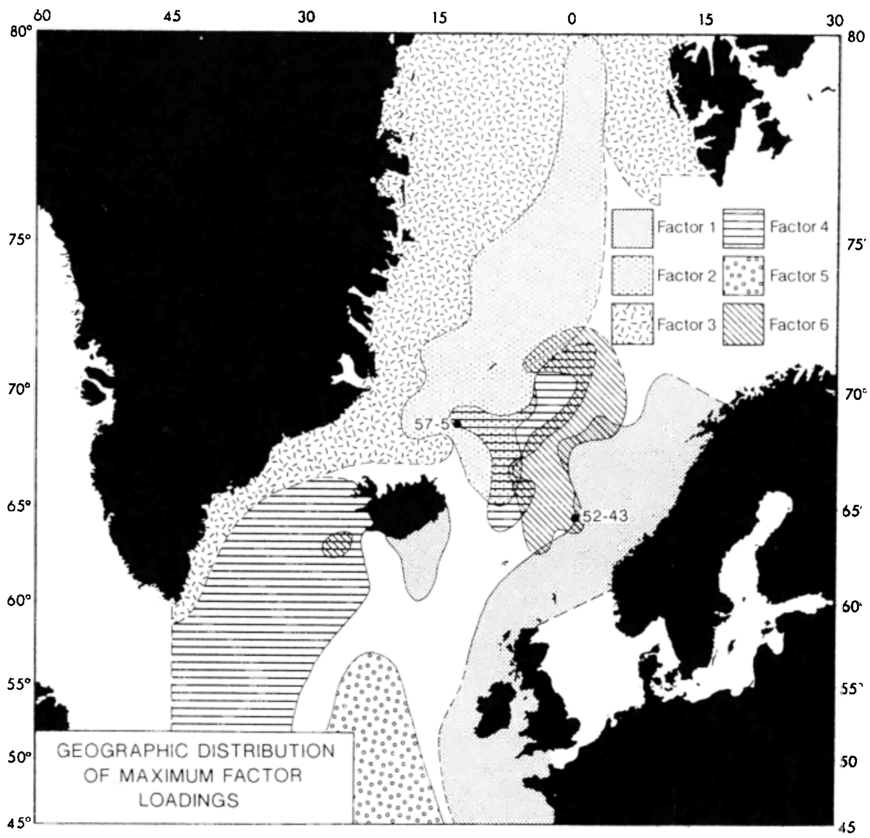

Fig. 8. Location of cores in relation to the present geographic distribution of maximum surface sediment diatom factor loadings. Note location of cores 57-5 and 52-43.

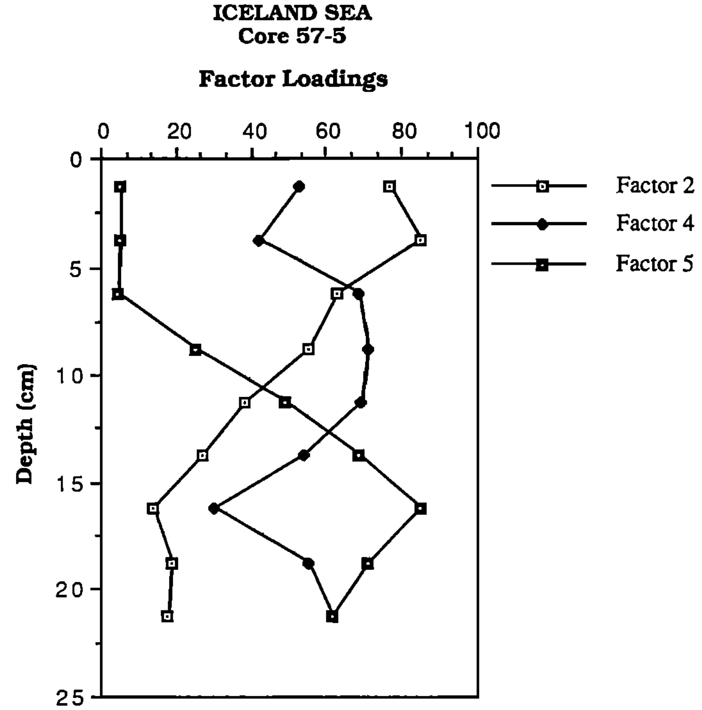

Fig. 9. Downcore Holocene variation of factor loadings (the Arctic Water assemblage, the Arctic-Norwegian Waters Mixing assemblage, and the Atlantic assemblage) in core 57-5 from the Iceland Plateau. Values plotted are factor loadings *100.

6.8°C, respectively. Core 52-43 records a 4.5° and 3.8°C (August and February, respectively) downcore temperature difference (Figure 10). This implies a higher downcore temperature variation for the Iceland Sea core which is in agreement with the modern presence of Arctic assemblages in the area.

DISCUSSION

The higher than modern temperature values observed in both the Iceland and the Norwegian Sea cores (Figure 10) correspond well with the continental climatic records from both sides of the GIN Sea, i.e., from Scandinavia and Greenland. The postglacial climatic optimum (hypsithermal) is especially well documented in the European continent. The paleoclimate record in Britain reconstructed from radiocarbon-dated beetle remains reveals a very marked improvement in climate during 10,500-9800 years B.P. [Atkinson et al., 1987] which is in agreement with the high temperatures recorded from the Norwegian Sea core beginning with the Vedde ash layer level (10,600 years B.P.). Glaciological studies from Scandinavia give evidence for a nearly complete melting of the ice sheets during the Holocene climatic optimum [Karlén, 1988; Nesje et al., 1990]. These ice sheets reformed about 2000 years B.P. in response to deteriorated climatic conditions. Kvamme [1984] argued that the Jostedalsbreen, western Norway, ice cap disappeared for some time prior to 5000 years B.P. on the basis of tree line studies. Upward displacement of the tree line in the Scandinavian mountains occurred between 9000 and 5000 years B.P. during optimal temperature conditions reaching higher than the present levels, and deforestration as a result of climatic detorioration took place about 5000 years B.P. [Simonsen, 1980; Berglund, 1983; Selsing and Wishman, 1984; Kullman, 1987]. The Holocene climatic optimum is well documented also in terrestrial pollen records of northern Europe. Forest communities were dominant 8000-4000 years B.P. in western Norway; thereafter a strong *Pinus* expansion occurred between 4000 and 3800 years B.P., indicating a shift to cooler temperatures [Berglund, 1983]. At Haugabreen, southern Norway, organic rich soils developed first at 5265 years B.P. [Caseldine and Matthews, 1987]. These authors tie the development of these soil horizons to a deterioration of the climate.

The climatic proxy data from the Greenland side of the GIN Sea show a similar climatic development. Ice core texture studies conducted on the Agassiz ice core from the Canadian Arctic islands indicate a maximum melting of the ice cap between 9000 and 7000 years B.P. [Koerner, 1989] corresponding to the time interval with highest temperatures in the Iceland Sea core (Figure 10). An extensive Holocene stratigraphy and vegetation history investigation conducted in the Scoresby Sund area, East Greenland, by Funder [1978] supports the Holocene diatom assemblage successions and accompanying temperature variations recorded in the Iceland Sea core (Figures 9 and 10). Glaciological data from the area shows an oscillatory retreat of major glaciers between 10,400 and 9400 years B.P., indicating fluctuations of climate during a period of general climatic improvement. This time interval

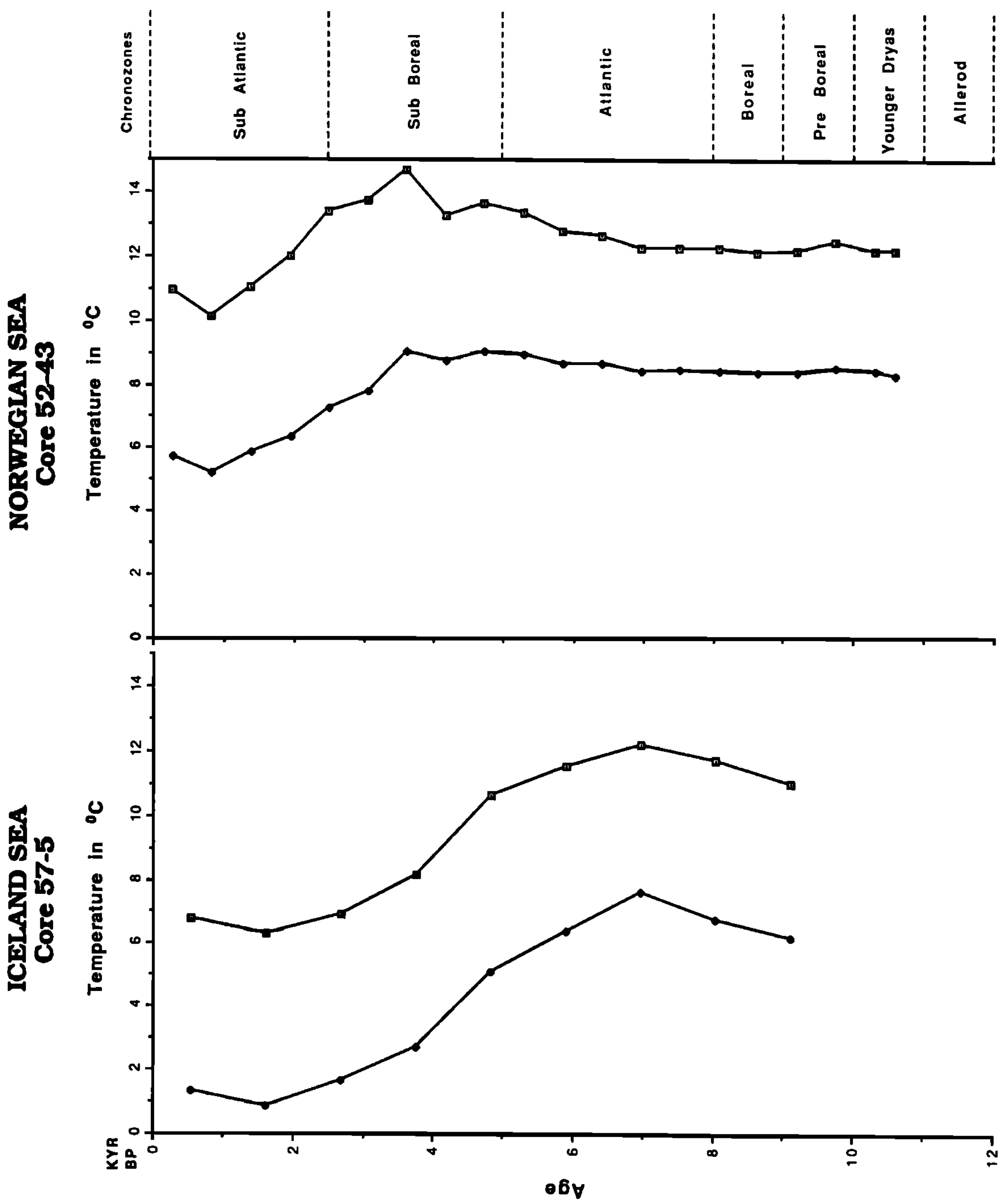

Fig. 10. Downcore Holocene August (open square with a dot, on the right) and February (solid square, on the left) sea surface temperature variations on the Iceland and the Norwegian Seas. Chronozones from Mangerud et al. [1974].

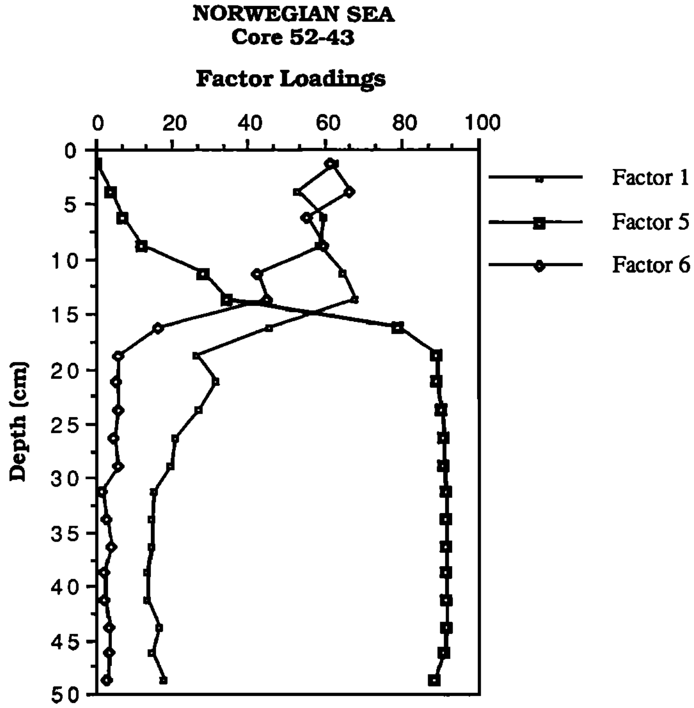

Fig. 11. Downcore Holocene variation of factor loadings (the Norwegian-Atlantic Current assemblage, the Atlantic assemblage, and the Norwegian-Arctic Waters Mixing assemblage) in core 52-43 from the Norwegian Basin. Values plotted are factor loadings *100.

in the Iceland Sea core does not contain diatoms, but the first sample (9100 years B.P.) with diatoms contains both the Arctic and the Atlantic diatom assemblages (Figure 9) together with some sea ice related species, supporting the general improvement and perhaps also the fluctuation of the climate during this time interval. Macrofaunal studies show the first appearance of the subarctic species *Pecten islandica* and *Mytilus edulis*, which are dependent on long warm summers for the development of their larva, at 8400 and 7700 years B.P., respectively, in the Scoresby Sund area [Funder, 1978]. Their appearance seems to correspond to the high temperature interval observed in the Iceland Sea core (Figure 10). The present occurrence of these species on the southeast coast of Greenland indicates a northward movement of the subarctic elements to the Scoresby Sund area during the early Holocene due to climatic conditions more favorable than the present in the area [Funder, 1978]. The pollen record of the area shows a sudden rise in continental *Betula nana* frequencies at circa 8000 years B.P. together with *Thalictrum*, indicating a general northward displacement of plant geographical borders and a climate warmer than the present [Funder, 1978]. The northward migration of these subarctic elements during the early Holocene parallels the northward shift of the diatom assemblages in the Iceland Sea. Disappearance of the subarctic macrofauna from the area and the appearance of high arctic *Salix arctica* soon after 5600 years B.P. and the reduction of *Betula nana* at 5100 years B.P. points to a decline in temperatures [Funder, 1978] consistant with the paleo-temperature curve of the Iceland Sea core.

On the north coast of Spitzbergen, the oldest *Mytilus edulis* shells found give a ^{14}C age of about 9400 years B.P. [Salvigsen and Österholm, 1982]. These authors also interpret the occurrence of the species in early Holocene as an indication for a climate warmer than today.

The rapid migration of *Betula* to southern Iceland at about 9000 years B.P. is also interpreted as an indication for annual mean temperatures that were higher than today [Simonarson, 1979].

The strong early Holocene influx of the warm Atlantic waters is also recorded from the marine realm. In the northwest Atlantic a major warming of the near-shore waters was registered around 10,000 years B.P. [Balsam, 1981]. The NW transect cores of Ruddiman and McIntyre [1981] show a maximum abundance of the planktonic foraminifer *Globorotalia inflata* between 9000 and 6000 years B.P. This abundance peak is interpreted by these authors as a period of strong influx of North Atlantic waters during the early Holocene. Paleotemperature estimates of Balsam [1981] and Kellogg [1975, 1984] based on planktonic foraminifera from the NW Atlantic and the Denmark Strait, respectively, support Ruddiman and McIntyre's [1981] interpretation of an early Holocene temperature maximum. Kellogg [1975] estimates early Holocene summer temperatures of 15.4°C from the Denmark Strait which is compatible with the Iceland Sea summer temperatures of 12°C (Figure 10) when the differences in latitudes are considered. A general decrease in SST and North Atlantic water intrusion is observed from about 6000 years B.P. to the present in the NW Atlantic [Balsam, 1981] and the Iceland Sea (Figure 10).

A shift in the benthonic foraminiferal fauna along the Norwegian continental margin [Sejrup et al., 1980] and in the macrofauna and planktonic foraminiferal fauna off northern Norway occurred around 9810 and 10,000-10,400 years B.P., respectively [Rasmussen, 1981; Andersen et al., 1982; Hald and Vorren, 1984; Thomsen and Vorren, 1986]. This change is marked by a considerable increase in diversity and a change from a low-arctic to a high-boreal fauna according to the above authors. Jansen et al. [1983] show evidence for warm water intrusion over the Norwegian continental margin around 10,000 years B.P. based on stable isotope data of the planktonic foraminifera and the general abundance increase of *Neogloboquadrina pachyderma* (right coiling). A zone with subtropical radiolaria between 7000 and 4000 years B.P. on the continental slope is interpreted as reflecting stronger influx of the North Atlantic waters into the Norwegian Sea by Jansen [1987].

In conclusion, the marine data from both the North Atlantic and the GIN Sea agree upon the warming of the surface waters starting around 10,000 years B.P. The Holocene optimal conditions (hypsithermal) seem to have influenced both the continental and the marine environment during the early Holocene around 9000-5000 years B.P. A climatic deterioration starting around 4000 years B.P. decreased the temperatures over both the surrounding land masses and the surface waters of the GIN Sea.

This study proves that diatoms have highly diversified assemblages which are affiliated with the physical properties of the surface waters in the GIN Sea. The diatom assemblages preserve the past temperature variations of the surface waters. There is also a very good correlation between the continental climatic proxy data and the geographic migration of the diatom assemblages. It is believed that detailed paleocirculation maps and paleotemperature curves for the GIN Sea could be produced through downcore diatom studies of strategically positioned and well-dated cores.

Acknowledgements. We thank J. Thiede and U. Struck of the Sonderforschungsbereich 313 of the University of Kiel, West Germany, for providing surface sediment samples and J. K. Ellingsen for drafting the figures. We are also grateful to M. Hald, E. Jansen, and two anonymous reviewers for critically reading the manuscript. This research was supported by Norges Allmennvitenskapelige Forskningsråd, NAVF-RNF. This paper is POC contribution 18 and SFB 313 publication 116.

REFERENCES

Abelmann, A., Freeze-drying simplifies the preparation of microfossils, *Micropaleontology, 34*, 361, 1988.

Andersen, B. G., F. Bøen, A. Rasmussen, K. Rokoengen, and P. N. Vallevik, The Tjøtta glacial event in southern Nordland, North Norway, *Nor. Geol. Tidsskr., 62*, 39-49, 1982.

Alekseev, A. P., and B. V. Istochin, Chart of constant current in the Norwegian and Greenland Seas, *Trans. Knipovich Polar Sci. Inst., 9*, 62-68, 1956.

Atkinson, T. C., K. R. Briffa, and G. R. Coope, Seasonal temperatures in Britain during the past 22,000 years, reconstructed using beetle remains, *Nature, 325*, 587-592, 1987.

Balsam, W., Late Quaternary sedimentation in the western North Atlantic: stratigraphy and paleoceanography, *Palaeogeogr. Palaeoclimatol. Palaeoecol., 35*, 215-240, 1981.

Befring, S., Submarine massebevegelser nordvest av Storegga utenfor Møre og Romsdal: En genetisk klassifikasjon av og en regional oversikt over de øvre deler av sedimentene i rasområdet, Cand. Sci. thesis, 95 pp., Univ. of Bergen, 1984.

Berglund, B. E., Palaeoclimatic changes in Scandinavia and on Greenland- A tentative correlation based on lake and bog stratigraphical studies, *Quat. Stud. Poland, 4*, 27-44, 1983.

Beyer, I., Senkvartær paleoseanografi i det sentrale Islandshav, Cand. Sci. thesis, 150 pp., Univ. of Bergen, 1988.

Caseldine, C. J., and J. A. Matthews, Podzol development, vegetation change and glacier variations at Haugabreen, southern Norway, *Boreas, 16*, 215-230, 1987.

Fairbanks, R. G., A 17,000-year glacio-eustatic sea level record: influence of glacial melting rates on Younger Dryas event and deep ocean circulation, *Nature, 342*, 637-642, 1989.

Fryxell, G. A., and G. R. Hasle, *Thalassiosira eccentrica* (Ehrenb.) Cleve, *T. symmetrica* sp. nov., and some related centric diatoms, *J. Phycol., 8*, 297-317, 1972.

Fryxell, G. A., and G. R. Hasle, The marine diatom *Thalassiosira oestrupii*: structure, taxonomy and distribution, *Am. J. Bot., 67*, 804-814, 1980.

Funder, S., Holocene stratigraphy and vegetation history in the Scoresby Sund area, East Greenland, *Bull Groenl. Geol. Unders., 129*, 1-65, 1978.

Gran, H. H., Die Diatomeen der arktischen Meere, 1, Teil: Die Diatomeen des Planktons, in *"Fauna Arctica", auf Grund der Ergebnisse der deutschen Expedition in das nördliche Eismeer im Jahre 1898*, Vol. 3, pp. 511-554, Jena, 1904.

Grant, W. S., and R. A. Horner, Growth responses to salinity variation in four arctic ice diatoms, *J. Phycol., 12*, 180-185, 1976.

Hald, M., and T. O. Vorren, Modern and Holocene foraminifera and sediments on the continental shelf off Troms, north Norway, *Boreas, 13*, 133-154, 1984.

Hasle, G. R., Some *Thalassiosira* species with one central process (Bacillariophyceae), *Norw. J. Bot., 25*, 77-110, 1978.

Hasle, G. R., and G. A. Fryxell, The genus *Thalassiosira*: some species with a linear areola array, *Nova Hedwigia, 54*, 15-66, 1977.

Hopkins, T. S., The GIN Sea; Review of physical oceanography and literature from 1972, *Saclantcen Rep.*

SR- 124, Saclant Undersea Res. Cent., San Bartolomeo in Galdo, Italy, 1988.
Horner, R. A., Do ice algae produce the spring phytoplankton bloom in seasonally ice-covered waters?, in *Seventh Diatom Symposium*, edited by D. G. Mann, pp. 401-409, Otto Koeltz Science Publishers, 1982.
Horner, R. A. (Ed.), *Sea Ice Biota*, 215 pp., CRC Press, Boca Raton, Fla., 1985.
Hurdle, B. G. (Ed.), *The Nordic Seas*, 776 pp., Springer, New York, 1986.
Hustedt, F., Die Kieselalgen Deutschlands, Österreichs und der Schweiz unter Berücksichtigung der übrigen Länder Europas, sowie der angrenzenden Meeresgebiete, in *Kryptogamenflora von Deutschland, Österreich und der Schweiz*, teil 1, edited by L. Rabenhorst, pp. 1-920, Akademische Verlagsgesellschaft, Leipzig, 1930.
Hustedt, F., Die Kieselalgen Deutschlands, Österreichs und der Schweiz unter Berücksichtigung der übrigen Länder Europas, sowie der angrenzenden Meeresgebiete, in *Kryptogamenflora von Deutschland, Österreich und der Schweiz*, teil 2, edited by L. Rabenhorst, pp.1-845, Akademische Verlagsgesellschaft, Leipzig, 1959.
Imbrie, J., and N. G. Kipp, A new micropaleontological method for quantitative micropaleontology: Application to a late Pleistocene Carribbean core, in *Late Cenozoic Glacial Ages*, edited by K. Turekian, pp. 71-181, Yale University Press, New Haven, Conn., 1971.
Jansen, E., Rapid changes in the inflow of Atlantic water into the Norwegian Sea at the end of the last glaciation, in *Abrupt Cimatic Change- Evidence and Implications*, edited by W. H. Berger and L. D. Labeyrie, pp. 299-310, D. Riedel, Hingham, Mass., 1987.
Jansen, E., and K. Bjørklund, Surface ocean circulation in the Norwegian Sea 15,000 B.P. to present, *Boreas, 14*, 243-257, 1985.
Jansen, E., H. P. Sejrup, T. Fjæran, M. Hald, H. Holtedahl, and O. Skarbø, Late Weichselian paleoceanography of the southeastern Norwegian Sea, *Nor. Geol. Tidsskr., 63*, 117-146, 1983.
Jouse, A. P., O. G. Kozlova, and V. V. Mukhina, Distribution of diatoms in the surface layer of sediment from the Pacific Ocean, in *The Micropaeontology of Oceans*, edited by W. R. Riedel and B. M. Funnel, pp. 263-269, Cambridge University Press, New York, 1971.
Kanaya, T., and I. Koizumi, Interpretation of diatom thanatocoenoses from the North Pacific applied to a study of core V 20-130, *Sci. Rep. Tohoku Univ., Ser. 2, 37*, 89-130, 1966.
Karlén, W., Scandinavian glacial and climatic fluctuations during the Holocene, *Quat. Sci. Rev., 7*, 199-209, 1988.
Kellogg, T. B., Late Quaternary climatic changes in the Norwegian and Greenland Seas, in *Climate of the Arctic*, edited by S. A. Bowling and G. Weller, pp.3-36, Univ. of Alaska, Fairbanks, 1975.
Kellogg, T. B., Late Quaternary climatic changes: Evidence from deep-sea cores of the Norwegian and Greenland Seas, *Mem. Geol. Soc. Am., 145*, 77-110, 1976.
Kellogg, T. B., Late-glacial - Holocene high-frequency climatic changes in deep-sea cores from the Denmark Strait, in *Climatic Changes on a Yearly to Millennial Basis*, edited by N.-A. Mörner and W. Karlén, pp. 123-133, D. Reidel, Hingham, Mass., 1984.
Kipp, N. C., New transfer function for estimating past sea-surface conditions from sea-bed distribution of planktonic foraminiferal assemblages in the North Atlantic, *Mem. Geol. Soc. Am., 145*, 3-41, 1976.
Koerner, R. M., Ice core evidence for extensive melting of the Greenland ice sheet in the last interglacial, *Science, 244*, 964-967, 1989.
Kullman, L., Sequences of Holocene forest history in the Scandes, inferred from megafossil *Pinus sylvestris*, *Boreas, 16*, 21-26, 1987.
Kvamme, M., Vegetasjonshistoriske undersøkelser, Breheimen-Strynn Konsesjonsavgjørende Botaniske Undersøkelser, edited by O. B. Meyer, pp.238-275, *Rapp. 34*, Bot. Inst., Univ. i Bergen, 1984.
Kvamme, T., J. Mangerud, H. Furnes, and W. F. Ruddiman, Geochemistry of Pleistocene ash zones in cores from the North Atlantic, *Nor. Geol. Tidsskr., 69*, 251-272, 1989.
Mangerud, J., The Allerød/Younger Dryas boundary, in *Abrupt Climatic Change- Evidence and Implications*, edited by W. H. Berger and L. B. Labeyrie, pp. 163-171, D. Riedel, Hingham, Mass., 1987.
Mangerud, J., S. T. Andersen, B. E. Berglund, and J. J. Donner, Quaternary stratigraphy of Norden, a proposal for terminology and classification, *Boreas, 3*, 109-128, 1974.
Mangerud, J., S.E. Lie, H. Furnes, I. L. Kristiansen, and L. Lømo, A Younger Dryas ash bed in western Norway and its possible correlations with tephra in cores from the Norwegian Sea and the North Atlantic, *Quat. Res., 21*, 85-104, 1984.
Maynard, N. G., Relationship between diatoms in surface sediments of the Atlantic Ocean and the biological and physical oceanography of overlying waters, *Paleobiology, 2*, 99-121, 1976.
Nesje, A., M. Kvamme, N. Rye, and R. Løvlie, Holocene glacial and climate history of the Jostedalsbreen region, western Norway; evidence from lake sediments and terrestrial deposits, *Quat. Sci. Rev.*, in press, 1990.
Paasche, E., Phytoplankton distribution in the Norwegian Sea in June 1954, related to hydrography and compared with primary production data, *Fiskeridir. Skr., Ser. Havunder., 12*, 11, 1-77, 1960.
Ramsfjell, E., Phytoplankton distribution in the Norwegian Sea in June, 1952 and 1953, *Fiskeridir. Skr., Ser. Havunder., 12*, 10, 1-40, 1960.
Rasmussen, A., The deglaciation of the coastal area NW of Svartisen, North Norway, *Bull. Nor. Geol. Unders., 369*, 1-31, 1981.
Ruddiman, W. F., and A. McIntyre, Northeast Atlantic paleoclimatic changes over the past 600,000 yrs., *Geol. Soc. Am. Bull., 145*, 111-146, 1976.
Ruddiman, W. F., and A. McIntyre, The North Atlantic Ocean during the last deglaciation, *Palaeogeogr. Palaeoclimatol. Palaeoecol., 35*, 145-214, 1981.
Salvigsen, O., and H. Österholm, Radiocarbon dated raised beaches and glacial history of the northern coast of Spitsbergen, Svalbard, *Polar Res., 1*, 97-115, 1982.

Sancetta, C., Distribution of diatom species in surface sediments of the Bering and Okhotsk seas, *Micropaleontology, 28*, 221-257, 1982.

Schrader, H., and R. Gersonde, Diatoms and silicoflagellates in the eight meters sections of the lower Pleistocene at Capo Rossello, *Utrecht Micropaleontol. Bull., 17*, 129-176, 1978.

Schrader, H., and N. Koc Karpuz, Norwegian-Iceland seas: Transfer functions between marine planktonic diatoms and surface water temperature, Geologic History of the Polar Oceans; Arctic Versus Antarctic, edited by U. Bleil, *Nato ASI Ser. C, 308*, 337-361, 1990.

Sejrup, H. P., H. Holtedahl, O. Norvik, and I. Miljeteig, Benthonic foraminifera as indicators of the paleoposition of the subarctic convergence in the Norwegian-Greenland Sea, *Boreas, 9*, 203-207, 1980.

Selsing, L., and E. Wishman, Mean summer temperatures and circulation in a south-west Norwegian mountain area during the Atlantic period, based upon changes of the alpine pine-forest limit, *Ann. Glaciol., 5*, 127-132, 1984.

Simonarson, L. A., On climate changes in Iceland, *Jökull, 29*, 44-46, 1979.

Simonsen, A., Vertikale variasjoner i Holocen pollensedimentasjon i Ulvik, Hardanger, *AmS Varia, 8*, 1-68, 1980.

Simonsen, R., The diatom plankton of the Indian Ocean Expedition of R. V. *Meteor* 1964-1965, *Meteor Forschungsergeb., Reihe D, 19*, 1-66, 1974.

Sjøholm, J., Kvartære askesoner og sedimenter på Islandsplatået: geokjemiske og sedimentologiske undersøkelser av kjerne 57-7, Cand. Sci. thesis, 139 pp., Univ. of Bergen, 1987.

Smayda, T. J., Phytopankton studies around Jan Mayen Island March-April, 1955, *Nytt Mag. Bot., 6*, 75-96, 1957.

Sundström, B. G., The marine diatom genus *Rhizosolenia*, Ph. D. thesis, 117 pp., 39 pl., Univ. of Lund, Sweden, 1986.

Syvertsen, E. E., Resting spore formation in clonal cultures of *Thalassiosira antarctica* Comber, *T. nordenskioeldii* Cleve and *Detonula confervacea* (Cleve) Gran, *Nowa Hedwigia, 64*, 41-63, 1979.

Thomsen, E., and T. O. Vorren, Macrofaunal palaeoecology and stratigraphy in late Quaternary shelf sediments off Northern Norway, *Palaeogeogr. Palaeoclimatol. Palaeoecol., 56*, 103-150, 1986.

Williams, K. M., Recent arctic marine diatom assemblages from bottom sediments in Baffin Bay and Davis Strait, *Mar. Micropaleontol., 10*, 327-341, 1986.

N. Koc Karpuz and H. Schrader, Geological Institute, Avd. B, University of Bergen, Allégaten 41, N-5007 Bergen, Norway.

(Received February 21, 1990;
revised May 29, 1990;
accepted May 30, 1990.)